TALLINN UNIVERSITY OF TECHNOLOGY
SCHOOL OF ENGINEERING
Department of Mechanical and Industrial Engineering

ADDITIVE MANUFACTURING IN THE JEWELRY INDUSTRY - DESIGN AND PRODUCTION

KIHTLISANDUSTOOTMINE EHETE TÖÖSTUSES - DISAIN JA VALMISTAMINE

MASTER THESIS

Student: Hira Das Akash

Student code: 194224 MARM

Supervisor: Kaimo Sonk, Lecturer

Tallinn 2021

AUTHOR'S DECLARATION

Hereby I declare, that I have written this thesis independently.
No academic degree has been applied for based on this material. All works, major viewpoints and data of the other authors used in this thesis have been referenced.

"26" May 2021

Author: signed digitally
/signature /

Thesis is in accordance with terms and requirements

"26" May 2021

Supervisor: signed digitally
/signature/

Accepted for defence

"....." May 2021

Chairman of theses defence commission: .....
/name and signature/

Non-exclusive Licence for Publication and Reproduction of GraduationTthesis[1]

I, Hira Das Akash (name of the author) (date of birth: "16" February 1990) hereby

1. grant Tallinn University of Technology (TalTech) a non-exclusive license for my thesis

Additive manufacturing in the jewelry industry - design and production

supervised by

Kaimo Sonk

1.1 reproduced for the purposes of preservation and electronic publication, incl. to be entered in the digital collection of TalTech library until expiry of the term of copyright;

1.2 published via the web of TalTech, incl. to be entered in the digital collection of TalTech library until expiry of the term of copyright.

1.3 I am aware that the author also retains the rights specified in clause 1 of this license.

2. I confirm that granting the non-exclusive license does not infringe third persons' intellectual property rights, the rights arising from the Personal Data Protection Act or rights arising from other legislation.

---

[1] *Non-exclusive Licence for Publication and Reproduction of Graduation Thesis is not valid during the validity period of restriction on access, except the university`s right to reproduce the thesis only for preservation purposes.*

signed digitally (*signature*)

"26" May 2021 (*date*)

Department of Mechanical and Industrial Engineering

THESIS TASK

Student: Hira Das Akash, 194224MARM

Study programme, main speciality: Industrial engineering and management, MARM

Supervisor(s): Lecturer, Kaimo Sonk, +372 620 3267

Thesis topic:

Additive manufacturing in the jewelry industry - design and production

Kihtlisandustootmine ehete tööstuses - disain ja valmistamine

Thesis main objectives:

1. To explore the manufacturability and strength analysis of complex geometric shape jewelry design.
2. Strength analysis of designed jewelry.
3. General guidelines for jewelry design and manufacturing.

Thesis tasks and time schedule:

No	Task description	Deadline
1.	Topic proposal and structure of the thesis	14.12.2020
2.	Preliminary background studies and concept generation	18.01.2021
3.	Designing for the jewelry model	17.02.2021
4.	Printing of jewelry model in 3D printer	02.03.2021
5.	Analyzing and modifying the design in comparison with the results	03.04.2021
6.	Physical testing and result analysis	17.05.2021

Language: English **Deadline for submission of thesis:** "26" May 2021

Student: Hira Das Akash signed digitally "26" May 2021
/signature/

Supervisor: Kaimo Sonk signed digitally "26" May 2021
/signature/

Consultant: …… …..... ".....” May 2021
/signature/

Head of study programme: …… ..... ".....” May 2021
/signature/

Terms of thesis closed defence and/or restricted access conditions to be formulated on the reverse side

CONTENTS

PREFACE 6
1. INTRODUCTION 7
2. PROBLEM STATEMENT 11
3. MARKET RESEARCH 15
3.1 3D printer comparison 18
4. CONCEPT GENERATION AND SELECTION 24
4.1 Concept generation 24
4.2 The manufacturing process and pitfall 29
4.3 Concept selection 39
5. TECHNICAL RESEARCH 42
5.1 Fused decomposition modeling (FDM) 42
5.2 Printer parameters 43
6. STRENGTH ANALYSIS 46
6.1 Yield strength 46
6.2 Compressive strength 52
6.3 Critical situation analysis 57
7. PHYSICAL TESTING 63
7.1 Pentagonal box specimen test 63
7.2 Lantern specimen test 66
7.3 Helix specimen test 68
7.4 Twisted shape specimen test 71
8. LED JEWELRY 74
SUMMARY 77
LIST OF REFERENCES 79
APPENDICES 83

PREFACE

The thesis topic was selected on the basis of the author's interest and several discussions with the supervisor. The author would like to thank thesis supervisor Kaimo Sonk, Lecturer, for his guidance, support, and comments in the whole journey.
The author would like to thank Professor Kristo Karjust, Programme director, for helping and guidelines for the thesis. In addition, the author is expressing his gratitude to Professor Martin Eerme, and Researcher Maarjus Kirs for their support during thesis work design and analysis.
The author would like to thank especially Jaanus Ehrlich for his tremendous help and technical support.

Additive Manufacturing (AM) is significant and constantly growing manufacturing technique. 3D modeling offers designing freedom in intricated design to the designers in the jewelry industry. Fused deposition modeling (FDM) has emerged as one of the most promising and cost-effective techniques for forming free-form parts using the desktop 3D printer. The traditional jewelry design and model making are still time-consuming and laborious work involving efficient drafting and handcrafting manufacturing skills. Nowadays, the demands are increasing in complicated shape fashionable jewelry which can be difficult in traditional jewelry making. Market research has been done on the market share of additive manufacturing in the economy and investigating the popularity of the desktop 3D printer in recent years in terms of sales units. However, no substantial study found the manufacturability of curved surfaces or geometrical shapes in desktop 3D printers.
The purpose of this study to explore the area of 3D printed jewelry design, investigate the manufacturability of complex geometric shapes and forms, and strength analysis. This study has been started with designing a jewelry model with general conceptions of basic geometric shape design. Then, the three-dimensional drawing has been done with CAD software SolidWorks to visualize the design. Next, a desktop 3D printer has been used for printing the designed model with Polylactic acid (PLA) material. The study demonstrates the manufacturability of complex geometric shapes using ANSYS analysis, and a physical tensile test has been performed for the 3D printed model by a universal testing machine. Eventually, this study experimented on LED jewelry manufacturing with a pentagonal box design and figured out the production difficulties in processes. A designer can incorporate this study result as general guidelines during the design and production of jewelry.

Keywords: Additive manufacturing, jewelry industry, design, production, guidelines.

1. INTRODUCTION

The additive manufacturing (AM) method is increasingly growing in various industrial sectors, while three-dimensional (3D) printing is beneficial for the consumer market. It offers design flexibility as well as environmental and ecological benefits. According to the standard ASTM F42 committee [1], additive manufacturing is defined as the "*process of joining material to make objects from the 3D model data, usually layer upon layer, instead of subtracting manufacturing methodologies.* "AM can produce parts with exceptionally intricated and complex geometries with minimal post-processing, with the least material waste, and appliable to a wide range of materials such as plastics and metals. The possibility of design freedom has generated broad interest to the designers and engineers to create unique products that can be mass-produced on a low-volume economic scale. AM technique can design conventional assemblies into a single dynamic assembly that could not be assembled using current processes. Furthermore, another proponent of AM technology is environmental and ecological benefits. AM technologies and methods are rapidly expanding in various manufacturing areas such as the automobile, medical, aerospace, and fashion industries [2].

Despite technological advances, jewelry making has remained relatively unchanged over time. Jewelry design and model building are also time-consuming and labor-intensive processes that involve advanced drafting and hand-crafting abilities. Sometimes, due to technical constraints, highly qualified technicians may not produce complex and complicated geometrical forms, such as those based on natural patterns, fractals, or mathematical algorithms [3]. Recently there has been growing attention in 3D printing that can be used to overcome these constraints. In addition, computer-aided manufacturing has been widely used to create and improve manufacturing processes. Numerous software such as Matrix 3D, Jewel CAD, Rhinoceros 3D, Blender, ArtCAM, Jewel Smith, and Jewel Space create a design and produce CAD models [4].

Figure 1. 1 Desktop 3D printer, Creality Ender-3 Pro. [30]

Over 100 different 3D printers are available commercially in the global market [5]. Among them, desktop 3D printers (Figure 1.1) are available that are relatively small and affordable. Industrial-scale 3D printers are proficient in producing a wide range of materials on a large scale. A different combination of additive manufacturing (AM) techniques and material can be used depending on the requirements of the applications [6]. In Table 1.1, Yap and Yeong (2014) summarized various AM techniques, mechanisms, and materials used to produce fashion products and jewelry based on Chua *et al*. (2010).

Table 1. 1. Summary of AM techniques [6]

AM Techniques	Mechanism	Material
Fused Deposition Modeling (FDM): A material extrusion of AM process in which material is selectively extruded through a nozzle	The thermoplastic filament is fed into an extrusion head and is heated to a semi-liquid state before it is extruded and deposited in thin layers from the nozzle.	1. ABS 2. PLA 3. Flexible PLA
Selective Laser Sintering (SLS): A powder bed fusion AM technique in which thermal energy selectively fuses a region of a powder bed	A CO_2 laser beam selectively melts or fuses a thin layer of a powder particle. Thus, powder serves as a built-in support structure.	1.Polyamide

Selective Laser Melting (SLM): A directed energy depositions AM process instead of sintering, powder melting occurs to build an object.	A high-powered laser beam is selectively directed to the powder surface, and the powder particles are melted to form solid metal.	1. Stainless steel 2. Titanium-based alloy 3. Nickel-based alloy 4. Aluminium 5. Copper
Stereolithography (SLA): A vat photopolymerization AM process in which liquid photopolymer in a vat is selectively cured by light-activated polymerization	The machine consists of a built platform immersed in a bath of liquid resin. A laser source selectively cures a thin layer of liquid UV curable photopolymer resin in a vat.	1. Polyethylene-like material 2. Polypropylene-like material 3.ABS-like material 4. Polycarbonate-like material
Poly Jet: A material jetting AM process in which droplets of build material are selectively deposited	A layer of liquid photopolymer is deposited from jetting head and immediately cures using UV light.	1.Multi-materials with a different hardness shore value

3D printed jewelry might be fabricated by a wide range of material options, like PLA, ABS, stainless steel and bronze, and other precious material like gold. The desktop 3D (Figure 1.1) FDM printer can extrude both PLA and ABS plastic. In jewelry manufacturing, the final parts can be produced with both direct and indirect 3D printing techniques. The direct technique of the metal powder bed selectively using energy sources like laser or electron beam. Conversely, the indirect 3D printing technique is used to produce the master patterns used for investment casting for final parts or directly produce a mold for casting [7]. Because of the cost involved, the former approach is still not widely used. Nevertheless, firms such as Shapeways and Immaterilize have begun printing jewelry directly from precious metal powders [3].

Many studies have been focused on developing a constitutive model that can predict the effects of building orientation and layer thickness of the printed parts [8]. The investigation on FDM printing parameters observed that raster orientation and air gap had a more significant impact on FDM material's tensile strength than others [9]. Many investigators examined different printing conditions with the standard test specimen.

However, little information about the strength of curved surfaces or the complex geometrical shape parts. The purpose of this study to explore the area of 3D printed jewelry design, investigate the manufacturability of complex geometric shapes and forms, and strength analysis. Furthermore, it may also revitalize by researching jewelry material optimization, design improvement, trial production of the design.

This study started with designing a jewelry model with general conceptions of basic geometric shape design. Then, the three-dimensional drawing has been done with CAD software SolidWorks to visualize the design. Next, a desktop 3D printer has been used for printing the designed model with Polylactic acid (PLA) material. Next, for finite element analysis, ANSYS software has been used to investigate the tensile, compressive, and critical situation analysis. Finally, a physical tensile test has been performed for the 3D printed model by a universal testing machine.

The foremost part of the thesis starts with the study's problem statement that brings out the previous research about 3D printing jewelry design in additive manufacturing and finds out research opportunities—stating the purpose of the thesis and possible areas for exploring further. Then the market research chapter describes the market share of additive manufacturing in the economy and investigating the popularity of the desktop 3D printer in recent years in terms of sales units. Moreover, portraying the available option and comparison of low-cost 3D printers in the current market. In this chapter, a summary of 3D printed jewelry in the present commercial market has been demonstrated. Next, the concept generation chapter explains generating design concepts step by step, from paper sketching to CAD model drawing. This chapter also brings out the pros and cons of manufacturing 3D models.

Furthermore, a selection matrix of design has been developed for the selection of the optimum design model. The technical research chapter describes the additive manufacturing technique and the printing parameters of desktop 3D printers. In the strength analysis chapter, strength analysis has been done for all designed models in ANSYS software. The results of the analysis provide the recommendation in designing jewelry models. In the following chapter physical tensile test is done with jewelry models, and the result is analyzed. After analyzing the results, the recommendation can be given to the designer who wants to design and print their jewelry. In the later part of the thesis, one jewelry model is designed with LED to demonstrate and explore the feasibility of manufacturing jewelry with LED.

2. PROBLEM STATEMENT

3D printing technology is extensively used in aerospace, medical, engineering, construction, automobiles, architecture, etc. [11]. The purpose of these studies to explore the area of 3D printed jewelry design. The traditional jewelry design and model making are still time-consuming and laborious work involving efficient drafting and handcrafting manufacturing skills. However, skilled technicians cannot create intricate and sophisticated geometrical shapes or patterns because of technological constraints, such as natural patterns, fractals, or mathematical algorithms [10]. The designing process starts with any CAD software to create STL files, a standard tessellation language for storing the information about surface geometry of 3D objects [3]. The STL files are then transferred to a machine for converting to G-code and giving the command to print the 3D model by different AM techniques. There are two methods, the first one is to print directly using precious metal, and the others, creating prototypes using plastic, wax, or rubber as printing material, afterward using them as a pattern in investment casting. The first method is still not popular though few companies offering direct printing using precious metal powder.

3D modeling offers designing freedom in intricated design to the designers. They can create any shape, type, size, and simulation of ornaments. In general, while purchasing jewelry from providers, they offer their own designed jewelry. With the changing of demand, the clients are want to print their idea design which can be difficult in traditional jewelry making. Some individual is creating their imagined design in different 3D modeling software. In present days, the desktop 3D printer is affordable for home users to print their own. However, the printing model in printers depends on different parameters such as material, layer thickness, temperature, support structure, etc. Individuals who want to do printing jewelry directly would prefer the desktop 3D FDM printer, and these printers can extrude both PLA and ABS plastic. Though 3D printing technology is an advanced technique for producing complicated or multi-material parts, the mechanical properties of the 3D printed part are not sufficiently studied [11]. Somireddy M et al. [8] developed a constitutive model for 3D printed parts that can predict the effects of building orientation and layer thickness on the material performance of the printed parts. Ahn SH et al. [9] investigated FDM printing parameters and observed that raster orientation and air gap had a more significant impact on FDM material's tensile strength than others. However, the compressive strength of FDM materials founded higher than the tensile strength, which had little impact on the build direction. The mechanical properties of ABS FDM models with different printing angles were studied by Es-Said OS et al. [12], including tensile

strength, modulus of rupture, and impact resistance. They discovered that the 0º printing angle had the greatest strength and impact resistance of all the other printing angles. Sook AK et al. [13] focused on understanding the impact of printing parameters such as layer thickness, building orientations, raster width, and air gap on the compressive strength of FDM parts. This study established a statistical predictive equation for determining the optimal parameter setting.

Tianyun Yao et al. [11] examined qualitative evaluations of the effect of printing angles on ultimate tensile strength (UTS) and constructed a theoretical model for the UTS of 3D printing materials. They printed standard test specimens for study with desktop 3D printer MakerBot Replicator and used PLA as a test material [11]. Although this study illustrated tensile strength of straight and flat surface area with different layers of thickness and printing angles, there is no substantial study about the curved surface parts or geometrical shapes. In jewelry design, the intricated geometrical shape and forms are used. The designer wants to create an aesthetically attractive design for 3D printing, which is quite complicated in a traditional method. Especially with a desktop 3D FDM printer and using PLA or ABS as an extruded material, the printing parameters such as layer thickness, the orientation of printing parts, infill density, temperature, and support structure are essential for quality printing. Inappropriate printing parameters could cause missing the parts details. Desired printing quality and details depend on the printing orientation and the tensile and compressive strength of the parts. A study can be conducted on the manufacturability of complex geometrical shapes and forms based on design complexity. The study could be about the manufacturability of curve shapes such as cylindrical, conical, rounded, helix, or twisted surfaces widely used in free-form jewelry design. It is also recommended to study their strength and visual outcomes in FDM techniques with PLA, ABS materials. These studies could provide a guideline to the jewelry designer who wants to print the designed parts with a desktop 3D printer. There is no study found about the minimum size measurement guidelines for printing jewelry that remains with its detailed design. This study might help assume a minimum range of size measurement of the printing parts in desktop 3D printers. The support structure pattern for the parts could be studied during printing, minimizing the finishing effort after printing. It plays a significant role in retaining the overhanging details of the design.

Kinematic jewelry design is a complex assembled parts of hinged, snap fits, ball-socket join that behaves as a moving element, coupling with links. Nervous System [16] designed such kinematics jewelry with hinged, customized designed triangular parts that move as a continuous fabric. The pieces of jewelry are built up layer-by-layer, slightly flexible nylon plastic using selective laser sintering [15]. However, the other

types of joint or mechanism are yet to study. This study will explore the free-moving link joint between the jewelry links and design for snap-fit joints.

Figure 2. 1 Kinematics by Nervous System. [40]

In current market trends, users prefer more innovative trends in jewelry design. Different online shops and designing companies are offering LED jewelry for the customers. Though this trend is not only limited to jewelry, even in dresses, pants, scarves, corsets, jackets, and shoes [14]. Cole Cordle, the owner of 'Light up your life LLC,' has been designed LED necklace, earrings since 2017 [14]. A study can be conducted about designing the jewelry with LED and examined the manufacturability in desktop 3D printers. This study can guide the designer about the flexibility of electrical devices and the suitability of designing parameters.

Figure 2. 2 LED earring (multi-color LED). [41]

Therefore, the purpose of this study is to investigate the manufacturability of complex geometrical shapes and forms, the strength of the printed parts, and the visual outcome of parts after the printing. This study will provide guidelines about the minimum printing size limitations in desktop 3D FDM printers using extruded plastic materials. This study will focus on a free-moving joint in between two links of the designed jewelry parts. Furthermore, as the current trend of including LED in jewelry is becoming popular, this study will explore the possibility of integrating LED into designed jewelry parts.

3. MARKET RESEARCH

The evaluation of Additive Manufacturing (AM) has an extraordinary over the past three decades. By the Wohlers Report 2016, the market of AM was expected to grow to more than $21 billion by 2020 [17]. 3D printing in the jewelry sector is used for rapid prototyping, jewelry models for the mold with lost wax, or complete direct jewelry using plastic and metal 3D printer. According to SmarTech Market Publishing, an American research firm, this market may reach $900 million in 2026, which is entitled in *"3D printing opportunities in the jewelry industry-2017: An opportunity analysis and ten-year forecast"* [18].

According to Wohlers Report 2016, AM industry, including all AM products and services worldwide, raised 25.9% (CAGR) to 45.165 billion in 2015, whereas, in 2014, the industry reached $4.103 billion with 35.2%(CAGR) growth. The growth of CAGR from 2013-2015 was 31.5%, and over the past 27 years, it is an impressive growth of 26.2% [19]. Wohlers Associates has been tracking the increase in sales of AM systems for metal parts for 15 years. In 2015, an estimated 808 metal AM machines were sold, with a growth of 46.5% compared to 550 metal AM machines were sold in 2014 [19]. In 2015, the desktop 3D printer's (sell for less than $5000) sales unit was significant as it increased by 69.7% to an estimated 278,385 machines. Though, in 2014 was 88.0%, with sales of 163,999 machines. Over the past four years (2012-2015), the average unit sales growth was 87.3% [19].

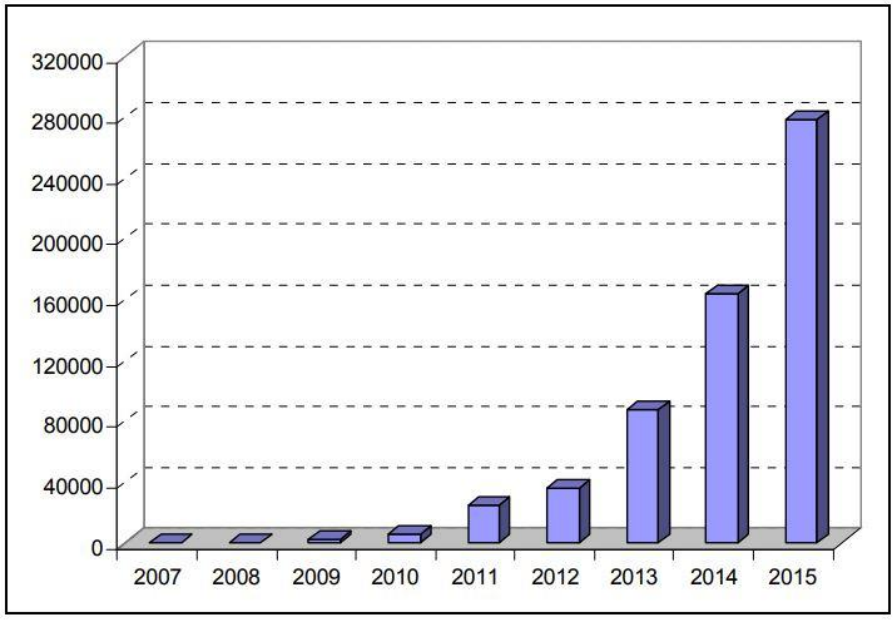

Figure 3. 1 The unit of sales 3D desktop machine from 2007 to 2015 [19]

The 3D printer market is rising. By the report of the Gartner group, in 2015, the 3D printers were sold at approximately 220,000, and the amount was almost doubled in 2016, approximately 450,000. They also forecasted that the number of sales could be increased to 6 million units in 2020[20].

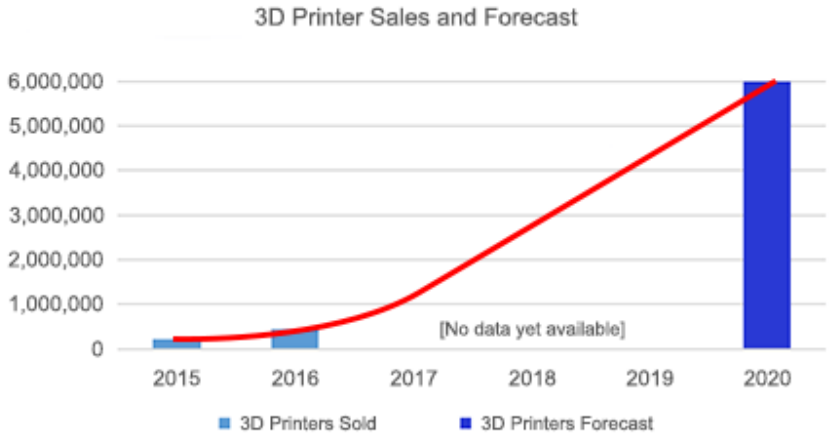

Figure 3. 2 3D printer sales and forecast [21]

According to the TransMagic, investigations were done by looking for top reviews of 3D printers in 2017 and compiled their comparison, therefore included into the comparison list highlighting critical features, showing in Figure 3.3.

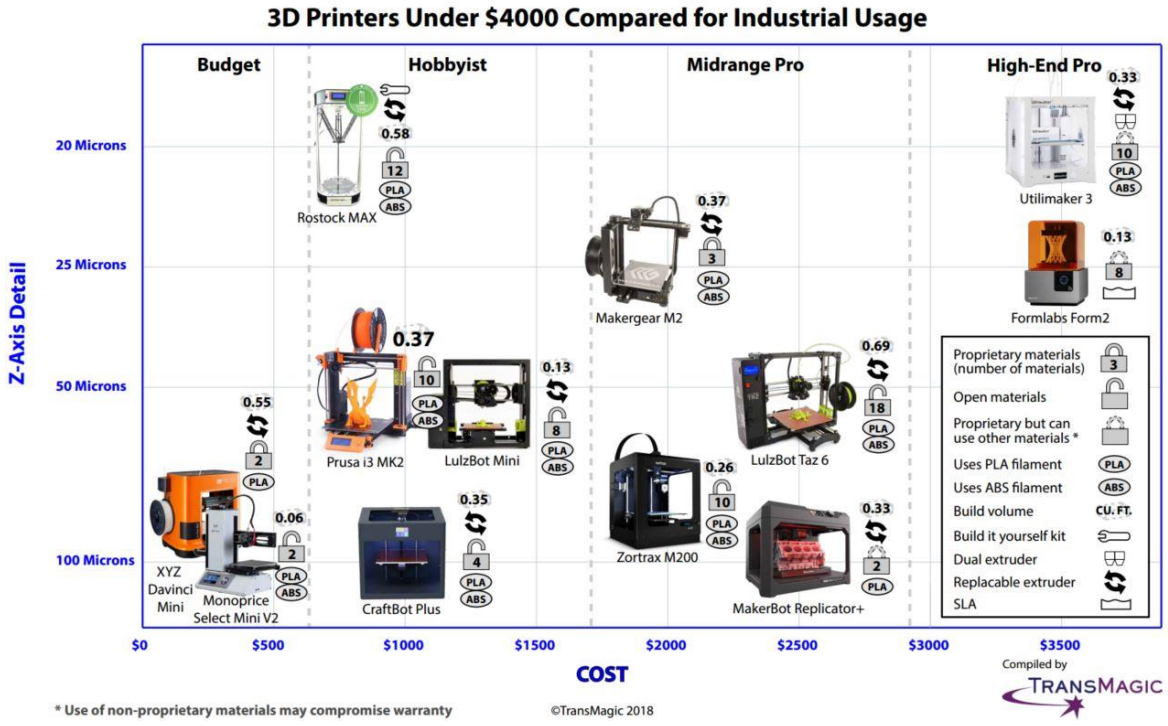

Figure 3. 3 3D printers under $4000 compared for industrial usage [21]

TransMagic categories the most popular 3D printers into four rough categories, which were economy (below $500), hobbyist ($700-$1200), midrange ($1800-$2500), and high-end (~$3500) [21]. In the vertical axis, the Z precision of the 3D printer was placed. The precision of the 3D printer ranges from 100 microns to 20 microns. The smaller number of microns will be a more precise and smoother surface finish. The total built volume ranges from 0.06 cf(cubic feet) to 0.69 cf, which is enough to print a coffee cup to print a basketball. Figure 3.3 indicates replaceable extruders options that show that the Makegear M2, the MakerBot Replicator+, the Ultimaker 3, Lulzbots Rostock Max, and the Craftbot Plus all have replaceable options. The Ultimaker 3 has a dual extruder head that allows the printer to build the model with two different materials or colors without replacing the filaments. In this chart, all the 3d printers can extrude PLA plastic, except the Makerbot Replicator+ and DaVinci Mini; others can also extrude ABS plastic. The Makerbot Replicator+ has options for an experimental extruder which allows a wide range of third-party material, but the rest of the printers are accepted only the proprietary material. The number is shown inside the padlock symbol, which indicates the total materials printable by each printer [21].

3.1 3D printer comparison

Each specific 3D printer can provide efficient quality with one material and inefficient quality with another material. So, it depends on the material properties adaptability of printers. Table 3 demonstrates the comparison of four 3D printers.

Table 3. 1 Comparison of 3D printers [22].

Picture				
Name	**Ultimaker 2+**	**Creality 3D CR-10S Pro V2**	**Creality 3D Ender 3 Pro**	**Monoprice Select Mini V2**
Price	$2500 approx.	$669 approx.	$280 approx.	$220 approx.
Overall Score(out of 100)	74	70	62	51
Pros	Excellent prints, ready to use from the box, widespread support	Efficient form factor, admirable prints of fused filament fabrication, easy to use	Great budget, solid printing capabilities, decent print quality.	Inexpensive, compact
Cons	Expensive	a bit more assembly than other printers	A bit difficult in ABS can require a bit of tinkering	Struggled with ABS, a small build area
Bottom Line	Best for who wants the best quality	High capability with quality at an affordable price	Authors favorite, tight budget with considering little tinkering to print perfectly	Not the best in this group, but affordable on a tight budget.
Print Quality(40%)	8 (out of 10)	7 (out of 10)	6 (out of 10)	5 (out of 10)
Ease of Use(30%)	7	7	6	5
Print Capabilities (20%)	7	8	7	5
Support (10%)	7	5	6	6

Build Volume (X*Y*Z)	223x223x205 mm	300x300x400 mm	200x200x250 mm	120x120x120 mm
Maximum extruder temperature	260ºC	260ºC	255ºC	250ºC
Maximum bed temperature	100ºC	110ºC	110ºC	60ºC
Included nozzle sizes	0.4mm installed (0.25mm,0.6mm, and 0.8mm included)	0.4 mm	0.4 mm	0.4 mm
Print layer height range	0.25mm nozzle:0.15-0.06mm 0.40mm nozzle: 0.2-0.02mm 0.6mm nozzle: 0.4-0.02mm 0.8mm nozzle: 0.6-0.02mm	0.1-0.4 mm	0.1-0.4 mm	0.1-0.35 mm
PLA?	Yes	Yes	Yes	Yes
ABS?	Yes	Yes	Yes	Yes
Network printing	No	No	No	No
SD card or USB drive	Yes	Yes	Yes	Yes

During the design process, the size of the 3D-printed jewelry can be easily managed. A designer may create the 3D CAD model and define or alter them following the CAD modeling software for individual customers [6]. Commercial CAD software like Solidworks, AutoCAD, PTC Creo, and Rhinoceros (Rhino 3D) is used in engineering, architecture, product design, and industrial design. SolidWorks is a hybrid solid and surface modeler, and Rhino 3D uses non-uniform rational B-spline (NURBS) in surface modeling. Rhino 3D is widely used to design fashion products like jewelry, where it does easy work with complex curved surfaces compared to SolidWorks [6].

Research by Statista Research Department shows that the 3D printing product and service are anticipated to exceed $40 billion by 2024 [23]. The present market offers 3D printable file-based websites to choose a free download or payment model. In addition, each site provides a wide choice of 3D printing designs to print at home. The

most popular sites for downloading 3D printable files are Thingiverse, CGTrader, Pinshape, Cults, MyMiniFactory, 3DExport, PrusaPrinters, GrabCAD Library, Free3D, and so on [24].

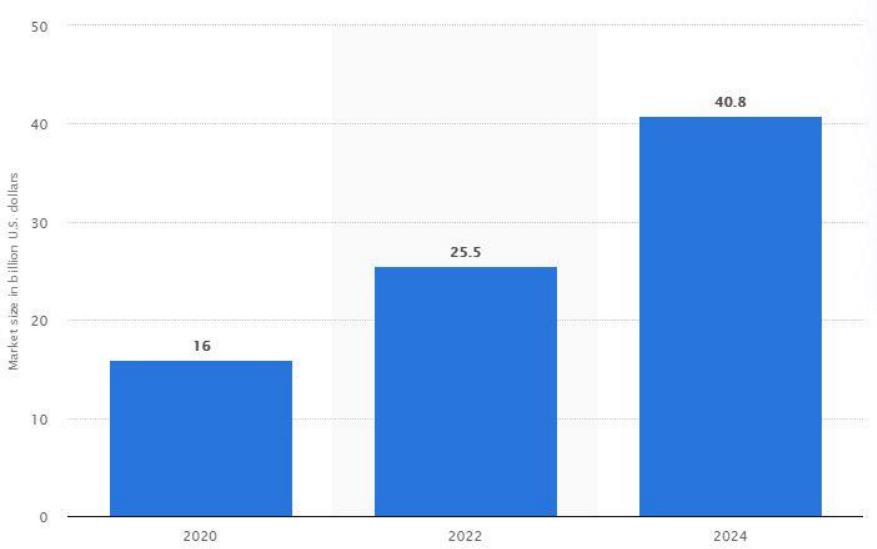

Figure 3. 4 The worldwide 3D printing product market size 2020-2024.[24]

Artists, artisans, and industrial designers have embraced AM techniques because of their ability to produce unique, fascinating, and attractive geometric shapes [25]. For example, in the jewelry industry, 3D printing is used for direct production and produces patterns for investment casting (Figure 3.5). 3D printing also creates freedom in new forms for clothing, shoes, purses, and other accessories in the fashion industry [25] (Figure 3.6).

Figure 3. 5 Jewelry produced with AM: Left- award-winning tiger ring from OG-Art-pattern printed in wax on a Solidspace machine[25]; Centre- Kinetic ring from Vulcan jewelry, courtesy of Vulcan jewelry; Right- custom R2D2 inspired ring from uptown diamond and jewelry- pattern printed in wax on a 3D system ProJet machine[26]

Figure 3. 6 AM in the fashion industry: Left- A dress collection of Iris van Herpen's Voltage haute couture, produced using laser sintering [27]; Center- Purse from Kipling, produced using laser sintering [28]; Right- Mutatio shoes by Francis Bitonti produced using SLS and then gold plated, courtesy of Francis Bitonti Studio.

The current 3D printing jewelry market pushes the previous jewelry elegance to another level. 3D printing jewelry is offering critical and intricated geometries that were rare to create in previous methods. By the 3D source, the investigation shows the best ten 3D printing jewelry from innovative companies worldwide [29]. 'Nervous System' is a 3D printing jewelry company that combines complex and unconventional geometries inspired by natural sources like coral, colorful agate slices, and more. One of the main philosophies of this company is crate online design applications that allow customers to collaborate and co-create products [29]. 'Radian' jewelry company is influenced by architecture and graphic design. They are creating stunning pieces out of stainless steel, gold, silver, and nylon. They have stock all around Germany, Europe, Middle East, Russia, and the USA [29]. Diana Law combines 3D printing and engineering with high fashion. This company creates stunning jewelry by selective laser sintering with materials like plastics, stainless steel, and nylon. Their 3D printed accessories are united with real precious gemstones like sapphires [29]. Guy and Max's company's philosophy stands the use of recycled metals where possible to avoid mining. The service is provided with a completely custom 3D design, intricate design and combine with any gemstone [29]. American Pearl using 3D printing to create precious geometric rings, earrings, necklaces, and more. They discovered that their sales go double after using the 3D printing process [29]. Anna Reikher creates her hand drawing design to turn it into 3D printed jewelry for the customers [29]. Studio Noesis offers intricate framework bracelets, rings, necklaces, and earrings with a simple, clean and shiny approach [29].

Table 3. 2 Summerize of a 3D printed jewelry company and their offers [29].

Company Name	**Description**	**Specialization**	**Offers to the customer**	**Example and Source**
Nervous System	Founder Jessica Rosenkrantz and Jesse Louis-Rosenberg in 2007.	Nervous system design, combined with unconventional geometries shape.	Collaborate and co-create products, besides jewelry, also offers lamps, innovative puzzles.	Source: [16]
Radian	Founded in 2012 by Nicole Nitz and Sandro Schieck. Based on Berlin company	Marvelous 3D printed jewelry pieces focused on geometric and abstract shapes. Sustainable production	The abstract and graphic shape necklaces, rings, bracelets, and earrings. Providing ring size conversion chart and return policy.	Source: [42]
Diana Law	Started 3D printed jewelry in 2014	Incorporated engineering with 3D printing.	Real precious gemstones, sapphires combine with ear maps, bracelets, and bags.	Source: [43]
Guy and Max	Founded by two brothers, the son of a diamond merchant in London	Recycle metals, design on customers' desire and dreams, collaborative process.	Custom pieces of jewelry and offers free yearly cleaning service after the purchase.	Source: [44]
American Pearl	The American company moved into the 3D printed jewelry in 2014	Customize and sophisticated design with gemstone and pearls with 3D printed jewelry	Allowing customers to customize their design via the web, choose the color and stones.	Source: [45]

Anna Reikher	A 3D designer from New York, United States	Inspired by nature, yoga, and origami.	The jewelry pieces are the result of hand drawing and customized.	Source: [46]
Studio Noesis	Founded by an Australian designer Luke Flanagan.	Intricated bracelet with a variety of materials including brass, silver, and bronze.	Offers lowest cost bracelet starts at below $100.	Source: [47]

4. CONCEPT GENERATION AND SELECTION

4.1 Concept generation

Jewelry items are used since ancient times to beautify the body. There are different types of jewelry to embellish every part of the human body, from a hairpin to toe rings. The popular types of jewelry are earrings, necklaces, bracelets, cufflinks, and rings. The primary idea generation for this study starts with the jewelry design, which can be manufactured with a small range 3D desktop printer. The primary design idea was about necklaces and bracelets. During the concept generation stage, the area selection of jewelry was considered both man and woman wearable design. Therefore, the preliminary design starts with paper sketching for bracelets design. The basic idea was to design flexible jewelry, a kind of different joints that can be manufactured in 3D printers.

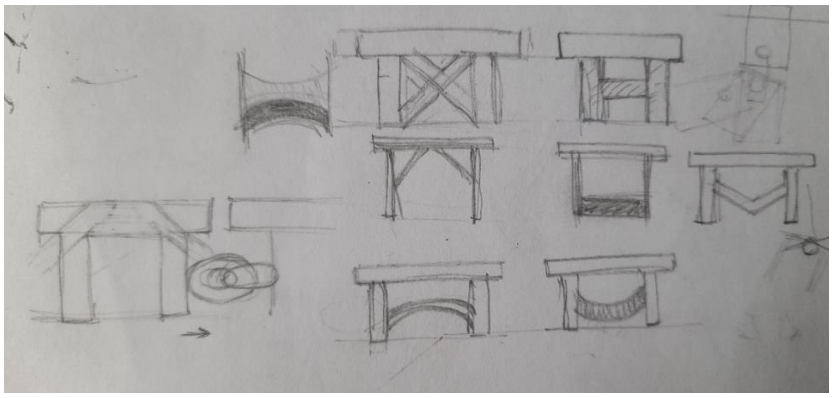

Figure 4. 1 Design of bracelet link in rectangular shape with different supports.

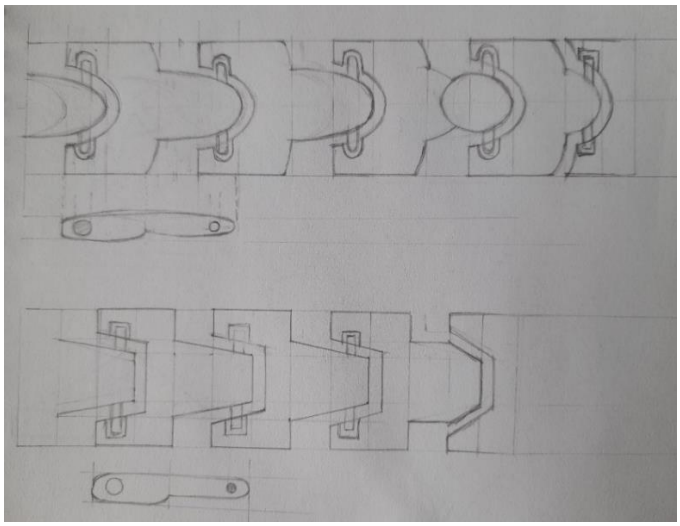

Figure 4. 2 Design of bracelet link in an irregular shape with integrated pin supports.

The possible design idea concerning connections in between subsequent links is generated in different mechanical ways. First, the joint between two links could be moved in a certain degree of freedom. Then the design might be flexible enough for laying on a curved surface. For example, Figures 4.3 and 4.4 illustrate a different idea about pin and hole joint between two links.

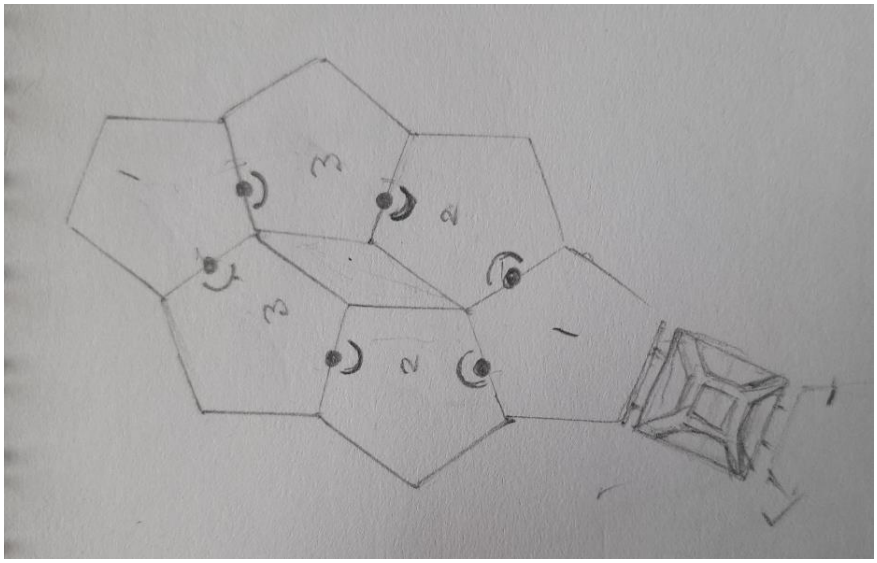

Figure 4. 3 Design of bracelet link in a regular shape with integrated pin and hole joints.

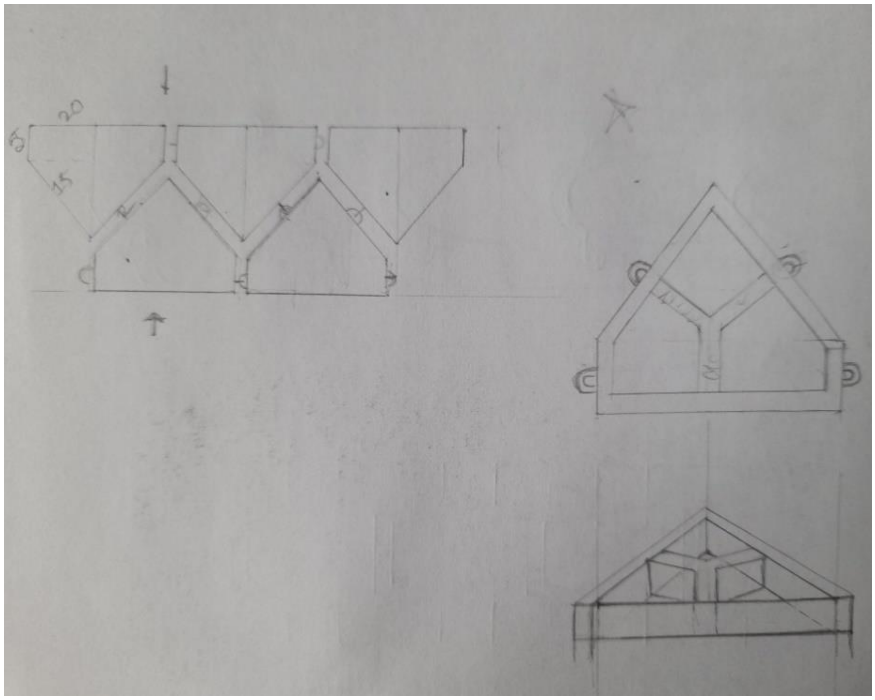

Figure 4. 4 Design of bracelet link in a regular shape with integrated spherical connections.

The designing idea also engaged some geometric shape formation. The basic idea is to create an interlinked geometric shape that makes a continuous chain as required. The

design should be considered flexible enough that it can be wear as a bracelet. Figure 4.5 illustrates the basic idea of a pentagon box shape link for the bracelet, an integrated connector to link up the following same links.

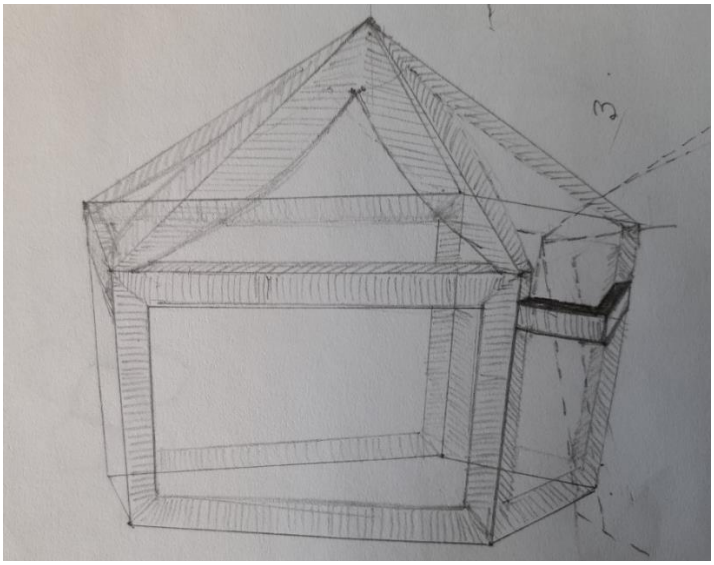

Figure 4. 5 Design of bracelet link in a geometric pentagonal box shape with integrated connector.

The design is also explored to figure out other geometrical shapes such as cylindrical, conical, spherical, helix, or twisted surfaces that can be included in designing bracelet links. The primary idea concept was generated from a conical-shaped object. Figure 4.6 illustrates the transformation of design for a different shape.

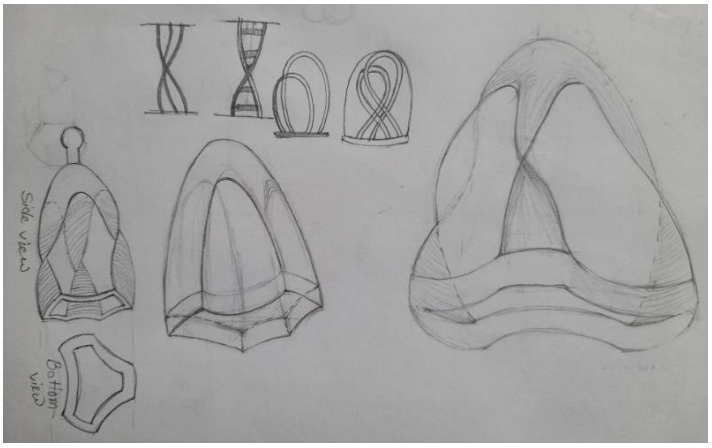

Figure 4. 6 Design of bracelet link with conical, cylindrical, helix, and twisted surface shape with integrated connector.

The designing processes start with a CAD software named SolidWorks student version software. Then, the designing process continues with different idea drawings and

creates the variation of support and linkage options. This rectangular design is close to the general pattern bracelet design, where it could be possible to design different types of impressions or stamps on the top surface. Five alternatives have been designed and assembled to visualize the outcome (Figure 4.7).

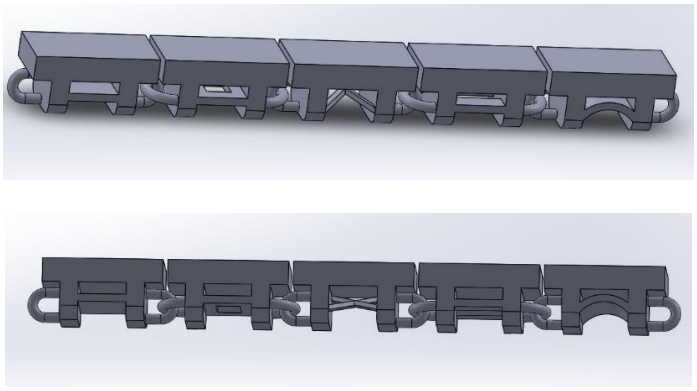

Figure 4. 7 Design of bracelet link in rectangular shape with different supports in SolidWorks software.

A possible modular design has been done with rectangular boxes, where boxes can be arranged to create an interconnected chain shape that can give a continuous chain shape. Also, it can create various rectangular shapes and rearrange along with different axis. In Figure 4.8, a modular design has been created with a chain shape.

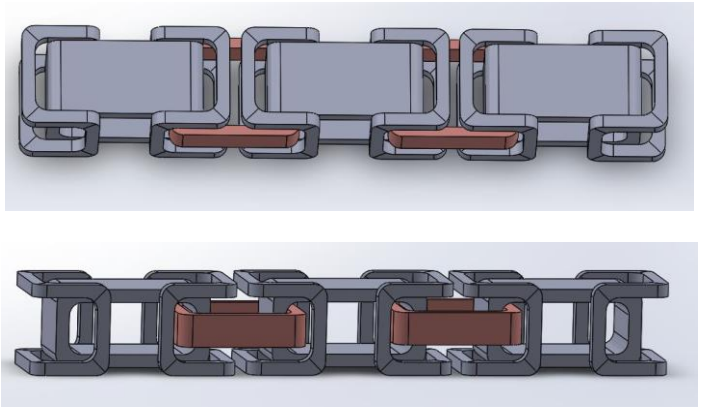

Figure 4. 8 Design of bracelet link in modular design with an interlinked connector in SolidWorks software.

Designing the concept of the regular geometric pentagon flat shape with an integrated spherical joint is shown in Figure 4.9. This design aims to create a 2D shape flat box with a spherical connector that will allow flexible movement and figure out the manufacturability of spherical joints.

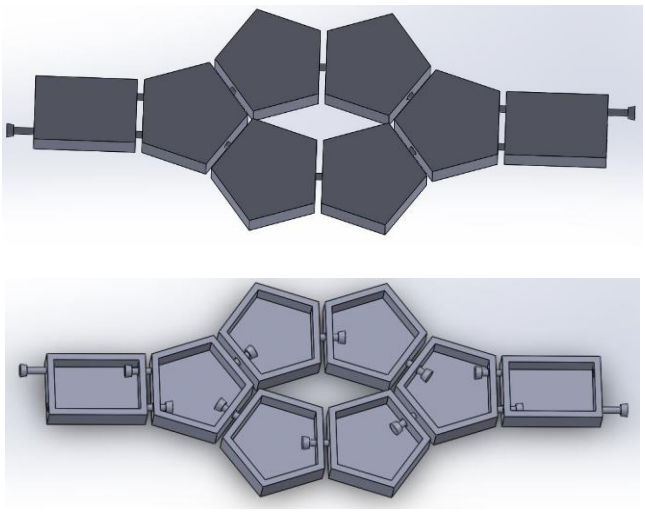

Figure 4. 9 Design of bracelet link in a pentagon flat shape with integrated spherical joints.

The designing of regular geometric box shape has been formed by a pentagon shape box with a pentagon top. This design also considers an internal connector extended edge to connect the subsequent links. The idea is to design a geometric box shape that has free space inside the box. This space can be used for any object that can move freely. Figure 4.10 illustrates the design for the pentagon box.

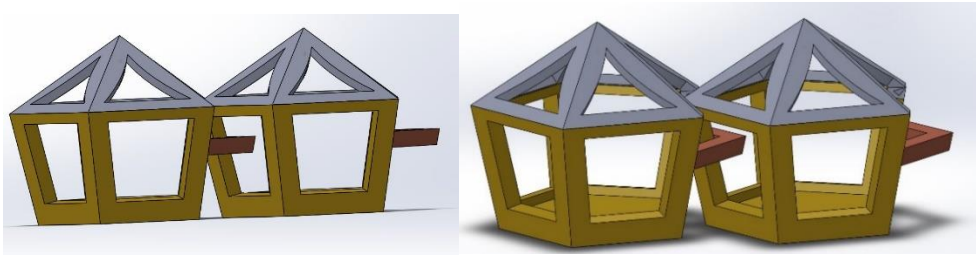

Figure 4. 10 Design of bracelet link in a geometric pentagonal box shape with an integrated connector in SolidWorks.

The design idea regarding the shape has a free-form shape, which can be redesigned with other shapes. To explore the different geometric shapes in design, cylindrical, spherical, conical, and twisting shapes are introduced in a lantern design shown in Figure 4.11. A sphere and ring connector is used to connect the two links internally.

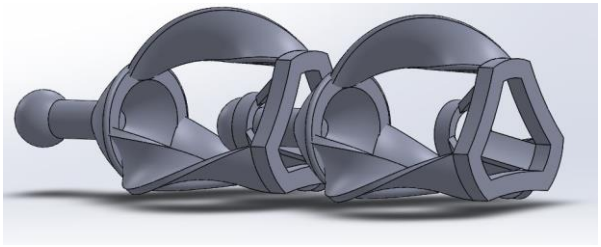

Figure 4. 11 Lantern design of bracelet link with conical, cylindrical, spherical, and twisted surface shape with an integrated ring connector.

Besides the twisting parts between the base and the upper conical shape, some different shapes are also constructed to fill up the gap between the two twisted shapes. Thus, four different shapes are included with the designed part, shown in Figure 4.12 (a - d).

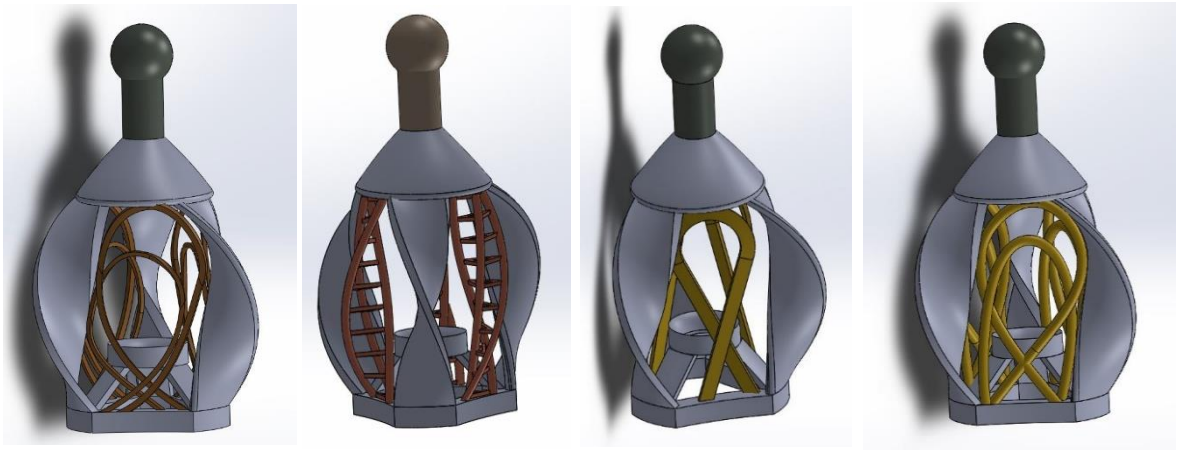

(a) (b) (c) (d)

Figure 4. 12 (a) Two rounded shape wire that twisted together and connected with the base of the design, (b) a helix shape three edge shape form connected within the base and upper part of conical shape, (c) a rectangular shape wire twisted and connected within the base and upper part of conical shape, (d) Two rounded shape wire that twisted together, and one wire criss-cross connected with the base of the design.

4.2 The manufacturing process and pitfall

After completing the possible design, the desktop 3D printer Ender-3 FDM printer [30] was chosen to print the models. The nozzle diameter of this printer is 0.4 mm with a printing accuracy of ±0.1 mm [30]. PrusaSlicer software [31] has been used for turning a 3D model into instructions for printing it. As the PLA material has been chosen for the printing models, the temperature of the nozzle and bed temperature was maintained at 210°C and 60°C, respectively. The layer height was 0.2 mm, and the speed was 60 mm/s [31]. The infill density was 95% with triangles fill pattern. The travel speed of non-print moves was 230 mm/s. The first model, the rectangular shape, was printed

with its designed measurement, 10 mm in XY axis orientation. The printing parameters were maintained the same as mentioned above. Figure 4.13 illustrates the printing outcome after separating the supports.

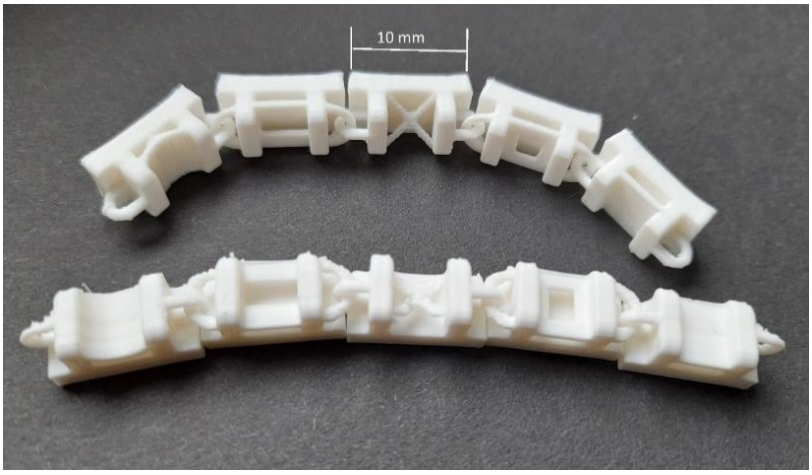

Figure 4. 13 The printing outcome of rectangular shape design after removing supports using Ender-3 FDM printer.

According to the printing outcome of rectangular shape, the key aspects are:

- The support under the overhanging part was difficult to remove.
- The printing outcome was found the actual shape according to design, though the connector (diameter 0.8mm) between two bars was printed with less strength. The printed shape less than 1 mm was found weaker and irregular shape.
- The outer surface smoothness was entirely satisfactory.
- The movement degree of freedom was convenient. However, there is an opportunity to improve the flexibility and degree of freedom of movement through a redesign.

The second model, a modular design, was printed with the same parameters. It was also printed in XY axis directions with auto-generated supports (Figure 4.14). The size of one link is 16 mm.

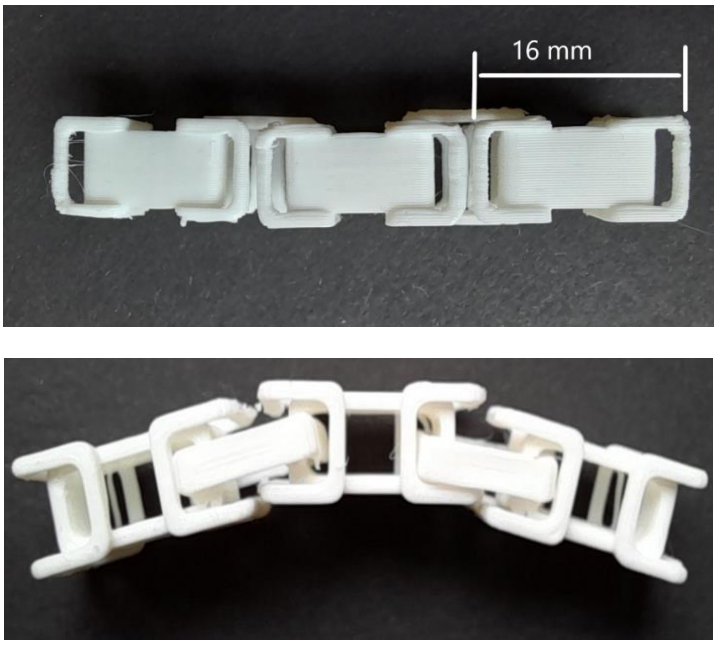

Figure 4. 14 The printing outcome of the modular design using the Ender-3 FDM printer.

According to the Figure 4.14 printing outcome of modular design, the key aspects are:

- The support under the overhanging part was challenging to remove as the size is less than 5 mm from the base.
- In XY-direction printing outcome was provided the actual shape of details according to the design. However, the small rectangular box which a wall thickness is 0.68 mm did not print with good strength.
- The outer surface smoothness was satisfactory, though it had some extra material layer in the side walls.
- The movement degree of freedom was suitable according to design. Still, there is an opportunity to improve flexibility.

The pentagon flat shape design print was continued with the exact parameters of the printer as declared earlier. It was printed in XY axis directions along with auto-generated supports (Figure 4.15). The edge of the pentagon shape was 14 mm, and the rectangular shape 15 mm.

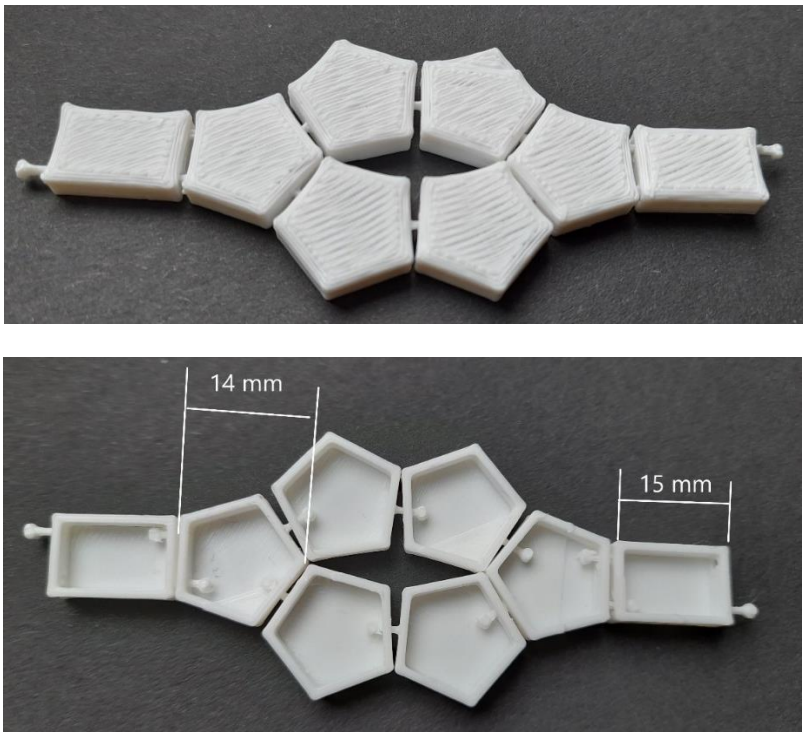

Figure 4. 15 The printing outcome of pentagon flat shape design after removing supports using Ender-3 FDM printer.

According to the printing outcome of pentagon flat shape design, the key observations are:

- The support was used almost less because of the flat geometric shape. However, under the pin part, it was challenging to remove the supports.
- The outer surface smoothness was relatively satisfactory, though it had some extra melted material in the hole part of the design.
- The pin-hole area restricted the movement of the interconnected pentagon shape, and there was a possibility to break easily.

The geometric pentagon box shape design was printed with defined parameters, and the height of the pentagon box was 12 mm in size. The support was auto-generated and was printed in XY directions (Figure 4.16).

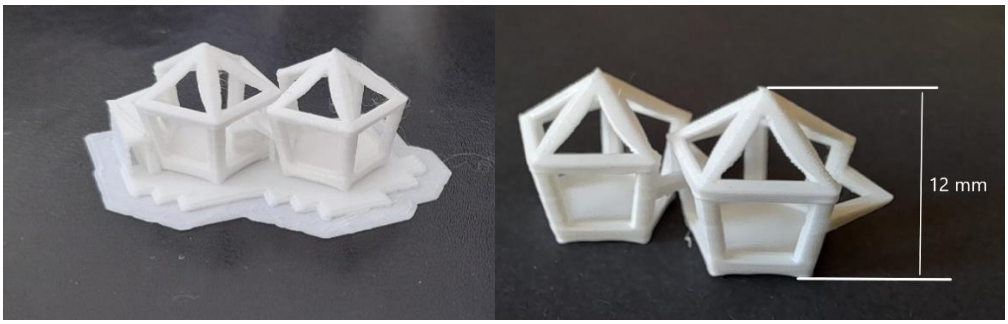

Figure 4. 16 The printing outcome of pentagon box shape design with supports (left) and after removing supports (right) using Ender-3 FDM printer.

The printing outcome provides the information about design's printability are discussed below:

- There was quite a lot of support under the overhang extended link, and it was tricky to remove the supports.
- In XY-direction printing was provided the actual shape of details according to the design.
- The outer surface smoothness was satisfactory.
- The side edge area restricted the movement of the interconnected pentagon box shape. However, there is an opportunity to improve the flexibility through a redesign of the extended part.

The last model, lantern design, was printed with a height of 19.5 mm in both Z and XY axis orientation. Again, the printing parameters were maintained the same. Figure 4.17 illustrates the printing outcome after separating the supports.

Figure 4. 17 The printing outcome of lantern design with supports (left) and after removing supports (right) using Ender-3 FDM printer.

According to the printing outcome of lantern design, the key aspects are:

- The helix part was not visible. The twisted part was not printed in the desired shape.
- The support around the helix and overhanging part was difficult to remove.
- Removing support from XY-direction printed part was challenging.
- The outer surface smoothness was not satisfactory.
- It was too small for printing in this size of the model. For that reason, printing quality was not desirable.

The study has experimented on the printing size of the lantern design as the details were not visible with actual scale. The printing was attempted with the same printer parameters and the size 28.5 mm (scale-up 150%) and 38 mm (scale-up 200%) illustrated in Figures 4.18 and 4.19, respectively. The printing outcome of the 28.5 mm lantern has been observed that the shape of the helix and twisted surface lost the continuity of material in some points. The removal of supports also remained difficult. In a 38 mm lantern, the twisted surface has been printed with a defined shape, and the helix shapes were printed sufficiently. However, during the removal of supports, some of the helix shapes were damaged. In different sizes of lantern design, the 38 mm has provided the desired printing outcome among all.

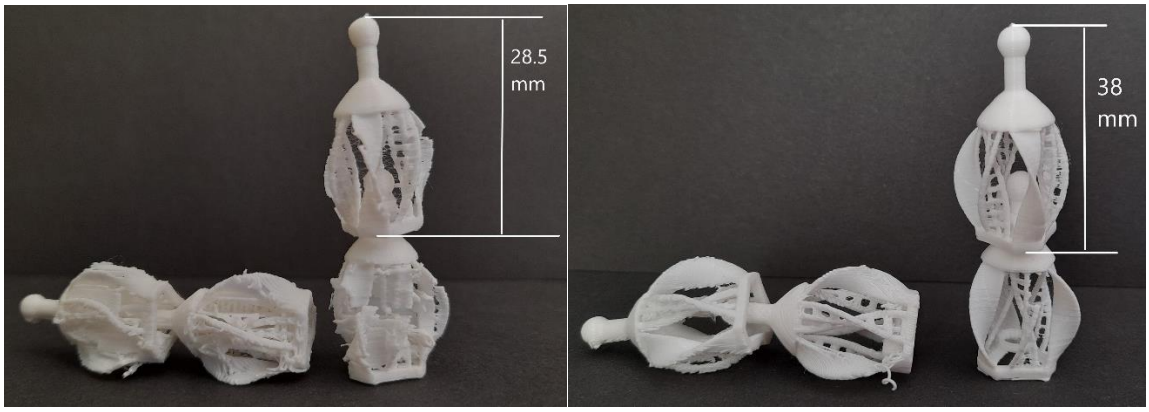

Figure 4. 18 The printing outcome of 28.5 mm lantern design (left) and 38 mm lantern design after removing supports (right) using Ender-3 FDM printer.

For comparing with the different 3D printers, MakerBot Replicator Z18 [32] has been chosen for two models, pentagon box and lantern design. This printer uses PLA as the material with 1.75 mm (0.069 in). The nozzle diameter is 0.4 mm (0.015 in). This printer uses its own MakerBot print software for operating printing parameters. During the printing, the layer height was 0.2 mm. The infill density was chosen 80% with a linear infill pattern. Extruder temperature was 210° C, travel speed 110 mm/s, and

printing speed was 40 mm/s. The support for the model was auto-generated. The MakerBot Slicer builds support under overhangs and long bridges. Figure 4.19 illustrates the printing orientations of two models where lantern design was positioned in both XY-axis direction and Z-axis direction. The pentagon box size was 12 mm, and the lantern design was 38 mm chosen for the printing.

Figure 4. 19 The printing orientation of pentagon box design and lantern design using MakerBot printer.

According to the printing outcome of pentagon box design (Figure 4.20):

- The support under the overhanging part was difficult to remove.
- In Z-direction, printing has provided the actual shape of details according to design.
- The outer surface smoothness was quite satisfactory.

Figure 4. 20 The printing outcome of 12 mm pentagon box design after removing supports using MakerBot printer.

According to the printing outcome of lantern design (Figure 4.21):

- The designed shapes were maintained better in the Z direction orientation than XY- directions.
- Removing support from XY-direction printed part was difficult, and the smaller detail design was lost during the cleaning processes.
- Moreover, in between two links, the rotation was limited due to the base part of the design.
- Removing support from Z-direction printed part was less complicated, but the small detail design parts were lost during cleaning.

Figure 4. 21 The printing outcome of 38 mm lantern design in Z-direction (left) and XY-direction (right) after removing supports in the MakerBot printer.

In both 3D printers, the auto-generated printing supports were causing the difficulties of removing the supports. Generated supports suppressed the helix of the lantern design. Manual support has been designed to come up with a possible solution to that problem (Figure 4.22a). The designed part was assembled in CAD systems with a clearance that did not attach to the lantern body. This manual support was placed in between two lantern links in Z-directions (Figure 4.22b). Then the printing has been done without allowing the auto-generated supports.

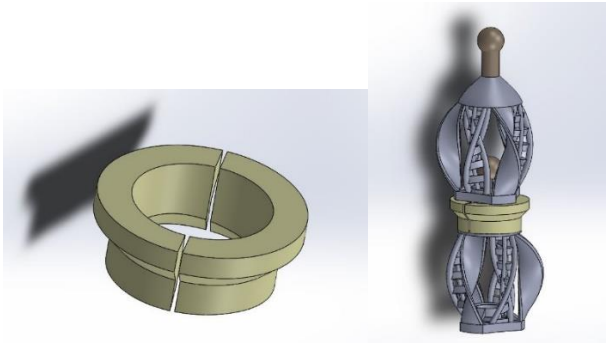

(a) (b)

Figure 4. 22 (a) The design of manual support as a part, (b) Assembly of parts with lantern design.

The assembly design was printed using Ender-3 with previous parameters. Figure 4.23 illustrates the printing outcomes of manual parts and after removing the support part. The manual part was printed with little support with the surface of the lantern body, which was easily removable manually. The helix part came out with the desired shape after the cleaning process.

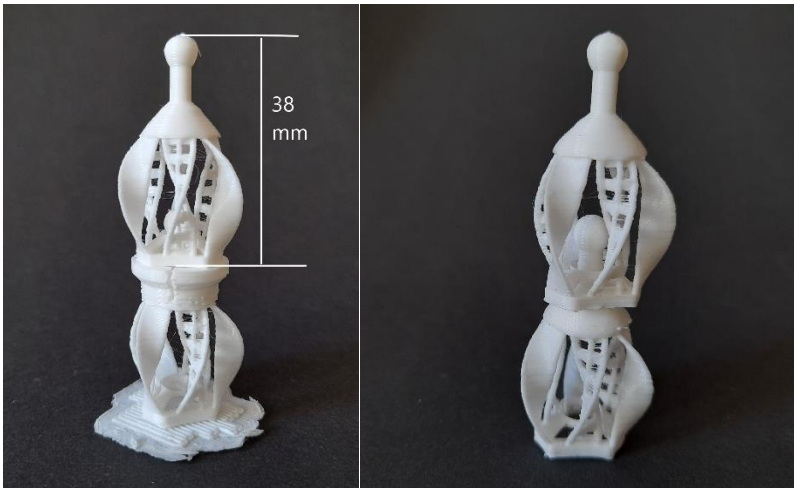

Figure 4. 23 The printing outcome of the lantern with designed manual supports (left) and after removing supports (right) using the Ender-3 FDM printer.

Figure 4. 24 The comparison between the auto-generated printing supports (left) and manual-designed printing supports (right).

In design improvement of lantern design, to increase the degree of freedom between two connected links, the distance between the base and middle circular ring has been reduced 3 mm to 1 mm. This change of design has allowed more freedom to rotate around the base. The designing idea also considers the different methods of joining the two lantern links. The assembled lantern part would be challenging to print more than

four links in Z-directions. Thus, the snap-fits joint has been considered in between the two link joints.

The diameter of the ring and the sphere's diameter were designed to push and fit inside together. Therefore, each link was printed separately and assembled by pushing the sphere head into the ring connections. Figure 4.25 shows the detailed view of a connection after printing. The connection was weak because the diameter of both ring and the sphere was the same. Thus it was easy to fit and detach with little force.

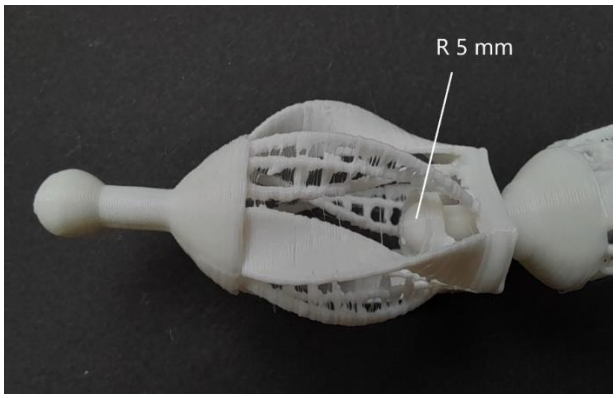

Figure 4. 25 The printing outcome of the lantern with snap-fits design with same 5 mm radius using Ender-3 FDM printer.

Another possible design has been done by cutting the sphere head and removing the material from inside that allows the head to push inside a smaller diameter than sphere diameter. However, the printing outcome was satisfactory, but the sphere head was broken when it pushes through the ring (Figure 4.26).

Figure 4. 26 The printing outcome of the lantern with snap-fits design with the cutting of sphere head using Ender-3 FDM printer.

The study designed further possibilities with additional lips on the ring to hold the sphere after passing through the ring to overcome the design difficulties. The ring diameter is more significant than the sphere diameter, and the lips diameter is smaller than the sphere diameter. The design is a non-detachable joint that allows fitting the sphere but will restrain the detachment from the ring. Figure 4.27 illustrates the CAD model of design and the manufactured parts of the designed model.

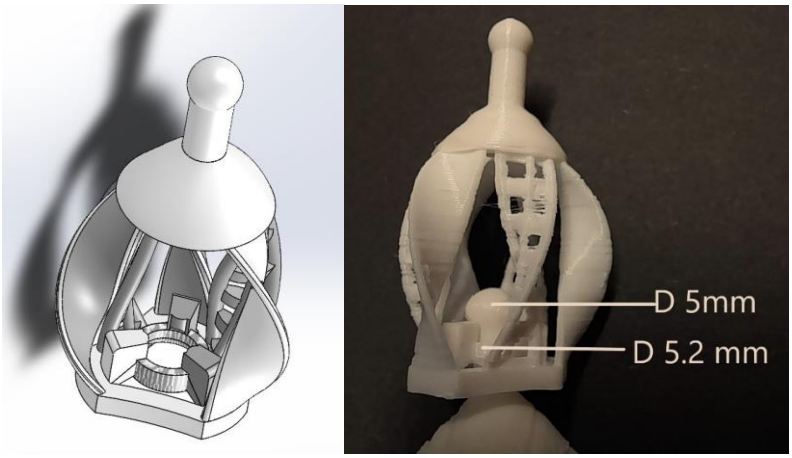

Figure 4. 27 The CAD design of snap-fits design(left) and printing outcome of the lantern with the snap-fits design using Ender-3 FDM printer(right).

4.3 Concept selection

The concept selection scoring matrix has been performed by selecting criteria. Five criteria have been selected according to the objective of the study. These criteria are discussed below:

The complexity of design: This study explores the different geometric shape complex designs and their manufacturability in desktop 3D printers. The shape with a simple rectangular, square, or flat surface could be a non-complex geometric shape. On the other hand, the shape with sphere, twisted surface, helix, incline triangle could be a complex geometric shape. The complex geometric shape and forms are desired to do a further continuation. The rating of less complex will be 1, and more complex will get 5 on a scale.

Surface smoothness: Surface smoothness means the level of outer surface roughness of a model. Depending on the surface curvature, the surface roughness varies during the printing process. This criterion is essential for the surface quality of the product. On a rating scale, 1 is for the rough surface, and 5 is for the smooth surface of the printed model.

Difficulties of removing supports: In a 3D printer, generating printing supports for the overhanging and unsupported parts is an important issue. However, removing the supports from the model after printing, generally a cause of damaging the details of models. So, fewer supports are always desirable for printing. Depending on difficulties in removing supports, 1 is more difficult to remove, and 5 is for least challenging to remove supports of the printed model.

Visual outcome of printed model: Aesthetics of design defines a design's pleasing qualities that include factors such as balance, color, movement, pattern, scale, and visual weight. The visual outcome might depend on the usability, functionality of attractive layouts. On a rating scale, 1 is least favorable, and 5 is most favorable.

Possibility of the new design: The further opportunities to introduce a new design or develop the existing design could be an option for developing a design. Depending on the implementation of a new design, 1 is the least possibilities, and 5 is for most possibilities of the designed model.

Table 4.1 shows the selection criteria with weight, rating, and the weighted score of all five designs used to decide a design for further development.

Table 4. 1 Concept selection matrix

		Concepts									
		Rectangular shape		Modular design		Pentagon flat shape		Pentagonal box shape		Lantern shape	
Section Criteria	Weight	Rating	Weighted Score	Rating	Weighted Score	Rating	Weighted Score	Rating	Weighted Score	Rating	Weighted Score
Complexity of design	30%	3	0.9	3	0.9	3	0.9	3	0.9	5	1.5
Surface smoothness	10%	2	0.2	3	0.3	4	0.4	5	0.5	3	0.3
Difficulties of removing supports	20%	3	0.6	4	0.8	4	0.8	3	0.6	2	0.4
Visual outcome of printed model	25%	4	1	3	0.75	3	0.75	5	1.25	4	1
Possibility of new design	15%	2	0.3	3	0.45	2	0.3	4	0.6	5	0.75
	Total Score	3		3.2		3.15		**3.85**		**3.95**	
	Rank	5		3		4		2		1	
	Continue?	No		No		No		Develop		Develop	

From the above selection matrix, among five designs, the pentagonal box and the lantern design are selected for further analysis as the most potential design. Although all selection criteria have been selected solely for this study, it is possible to choose other criteria upon the designer's own choice and consideration. Thus, depending on different design aspects, this selection matrix (Table 4.1) can be reconstructed. For this study, the complexity of form and the possibility of the new design have been considered. However, for the other designer, the selection could be modified.

According to the concept generation process, this study has explored different geometric designs from a sketch on paper to a printed 3D model to investigate the manufacturability of desktop 3D printers. The design with a dimension less than 10 mm has been found relatively infeasible to print with its actual detailed design. In lantern design with helix and twisted shape are found manufacturable in a minimum of 38 mm length size. Snap-fits design has been applied to the lantern design with satisfactory outcomes. The design parameters of snap-fits components are important for consideration. This design feature could allow the flexible assembly option. It is recommended to select the printing direction in XY direction rather than Z direction for the design to achieve the better strength of the model. The designer should consider the printing direction during the designing stage. This study also found difficulties with removing the auto-generated supports after printing. Designing manual supports in the model could provide an opportunity to ignore the auto support by the slicer software. It would be recommended for the designer to think about the possible manual support design for the designed model to minimize the auto support during 3D printing., A high-quality 3D printer is recommended to achieve better printing quality and strength of complex design.

5. TECHNICAL RESEARCH

5.1 Fused decomposition modeling (FDM)

The FDM is an additive manufacturing process in which thin plastic filaments create structures by layering them together. The FDM was patented by Scott Crump in 1988 [33] and commercialized by Stratasys in the USA. The filament is normally heated to a molten state before being extruded through the 3D printer nozzle. Then, according to the G-code instructions, the nozzle head travels three degrees of freedom to deposit the extruded polymer on the build plate. Figure 5.1, the principle of the FDM process illustrates in a schematic diagram.

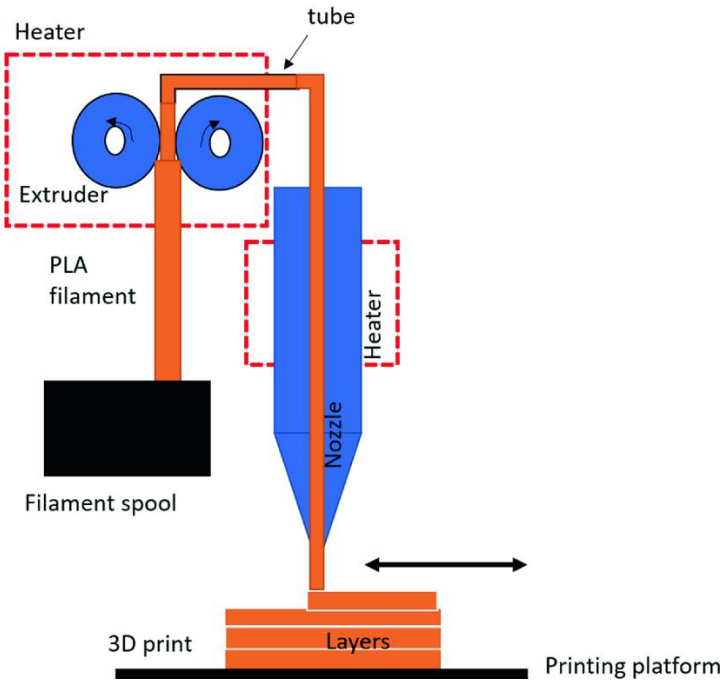

Figure 5. 1 Principle of fused decomposition modelling [34].

The material comes on a spool from a roll of plastic filament. To create a component, the filament is fed into an extrusion head and heated to a semi-liquid state. The head precisely extrudes and guides the molten material onto a fixtureless surface in ultra-thin layers. The flow of molten material can be turned on and off using a controlled process in the nozzle [35]. During the layering, the printing nozzle moves back and forth according to the spatial coordinates of the initial CAD model within the G-code files until the specified size and shape of the component are produced. In some FDM 3D printers, multiple extrusion nozzles can be used to deposit the polymer ingredients, particularly when compositional gradients are needed. For model material and support material, two different nozzles are used. Support material (SR30-XL) for the Stratasys uPrint-SE

system is water-soluble, while the model material (P430XL) for the same system is insoluble [35]. Therefore, the model and support material can easily be separated by exposure to water. A heated environment is maintained (at approximately 72°C) during prototyping to avoid structure tension and warping due to the filament cooling process.

In particular, most low-cost FDM 3D printers can only print one kind of thermoplastic, which is polylactic acid(PLA). PLA is a bioplastic that is both environmentally sustainable and safe for human and animal welfare. PLA is made from 100% sustainable materials, including corn, sugarcane, wheat, or other high carbohydrate resources [36]. The most low-energy and cost-effective 3D printer can extrude it because of transitional glass temperature between 50 and 70°C and a melting point temperature between 180 and 220°C [37]. PLA has been shown to have strong flexural modulus, tensility, and flexural strengths in its semi-crystalline form. PLA is offered in a range of colors and textures in the marketplace. Color PLA makes appealing to consumers, including those who work with domestic and decorative 3D printers. The variety of colors and textures of PLA has broadened the demand for CAD designers and toy fans. As a result, the designer can develop creative ideas and upload them to different databases such as TurboSquid, CG Trader, Shapeways, Cults3D, 3DSquirrel, and Thingiverse. The hobbyist and toy enthusiasts can purchase, download, and print the design on their own. Other material options can also be found in FDM processing, including polycaprolactone (PCL), polypropylene (PP), polyethylene (PE), polybutylene terephthalate (PBT), Acrylonitrile butadiene styrene (ABS), wood, nylon, metals, carbon fiber, graphene- doped PLA.

5.2 Printer parameters

A slicer converts a 3D model into printing instructions. Without a slicer, the printer would not be able to know about the instructions. Cura, PrusaSlicer, and Simplify3D are some popular slicers in the market [38].

Temperature is a critical parameter for 3D printers to produce quality prints because it affects every part of the printing process. For example, a nozzle temperature that is too low can cause under-extrusion and nozzle jams, whereas a too high temperature can cause over-extrusion, heat creep, oozing, and zits. Depending on the filament material and producer, PLA generally printed at a nozzle temperature of 180-220°C. The nozzle temperature for ABS and PETG are slightly higher, at 220-250°C and 220-245°C, respectively [39].

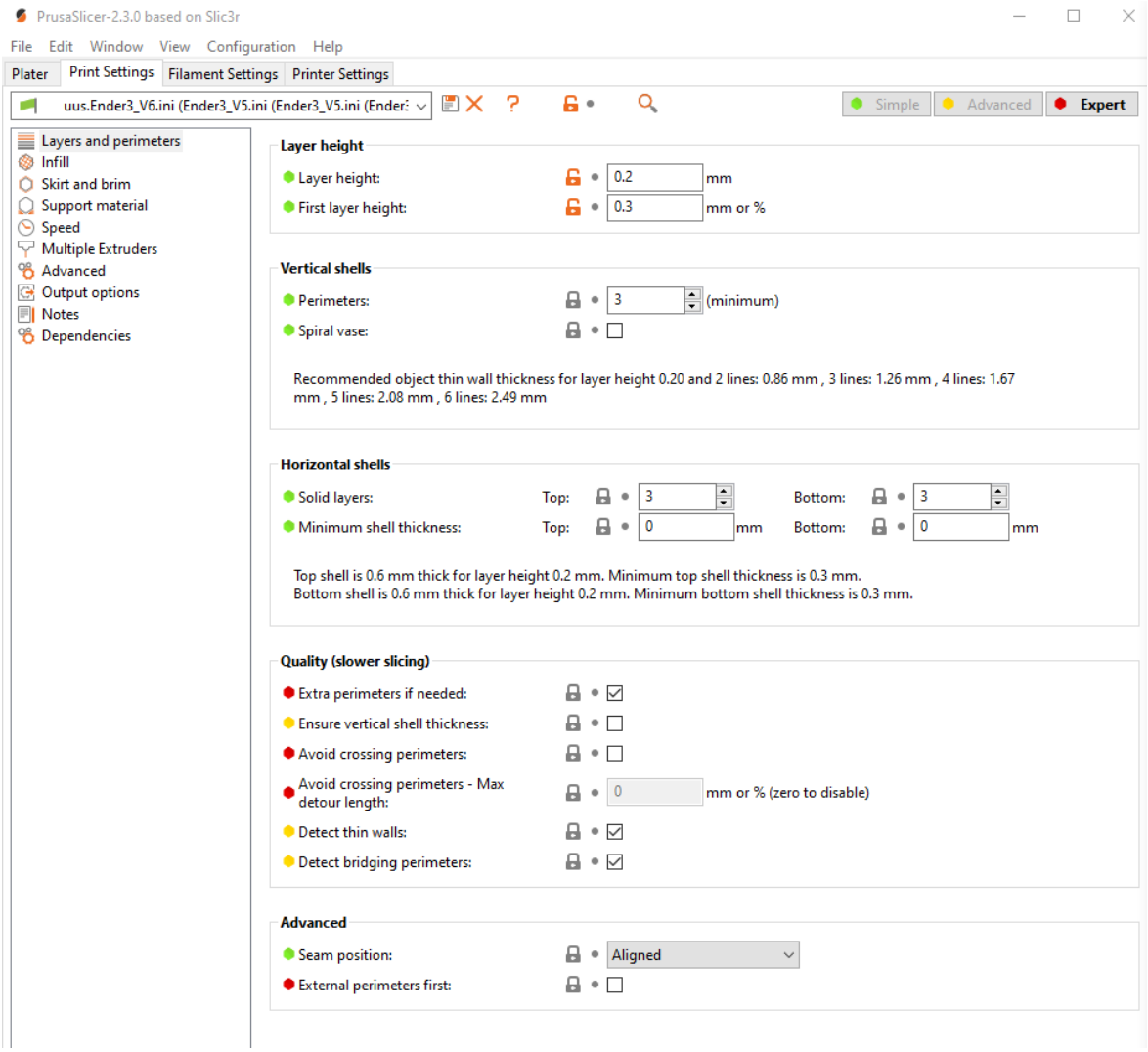

Figure 5. 2 An user interface of PrusaSlicer for printing parameters.

Bed temperature is essential for model printing, affecting how well a model sticks to the build plate. For example, PLA is comfortable with a bed temperature up to 60°C, whereas ABS needs a temperature range of 80-110°C with an enclosure to keep surrounding heat.

Layer height is another influential factor that means the distance the Z-axis moves up every layer. A detailed part can be achieved by a smaller layer height, and for the robust parts, a larger layer height is required. For example, a 3D printer like Ender-3, 0.2 mm layer height, is good. However, it is recommended to use 0.16 mm for intricate parts, 0.24 mm for more robust parts [39].

Speed is a vital parameter for printing, the speed at which the printhead moves. Printing too fast will result in under-extrusion and rough prints, while printing too slowly can result in hot and clogs (heat creep). For Ender-3, a safe printing speed is 60 mm/s for

PLA [39]. For the different sections of the parts like perimeters, infill, bridges, solid fill, support material, and gap fill, it is suggested to use 50-60 mm/s speed. However, the first layer should print with a speed of 20 mm/s for good bed adhesion. To determine how fast the printer moves during non-printing moves, known as travel speed. It has been recommended to use a travel speed of 130 mm/s for Ender-3 [39].

Retraction is the method of pulling the filament back while the printhead is not printing to prevent the excess filament from oozing out of the hot end. The retraction distance and speed can be used to regulate retraction. For example, for PLA and ABS, the suggested retraction distance is 5 mm for Ender-3, and the retraction speed for PLA is 40 mm/s, whereas, for ABS, a speed of 45 mm/s is recommended.

Infill setting is affected by both the strength of parts and the time it takes to print. For a stronger part, the high infill rate is applied usually increases the print time, while print time is reduced with softer ones. A complete solid part refers to 100% infill, and 0% infill is hollow. PrusaSlicer offers a range of infill pattern choices, including grid, triangle, gyroid, star, cubic, honeycomb, and more.

Shell or perimeter is the solid periphery and exterior of a printed part. The thickness of the shell is typically defined in millimeters or as many layers. Shell thickness is significant because of the strength of the model. Therefore, it is recommended to set the vertical, top, and bottom shells all of three [39].

Supports keep up overhanging features on models whether they follow particular criteria set by the slicer. Slicer software adds supports to the model where necessary. Those supports can be removed while the whole model is done.

6. STRENGTH ANALYSIS

The researches in this study have been designed to test all model that printed on the 3D printer. The study aims to test the structure of models, the yield strength, the compressive strength, and analyze some critical situational strength. Finite element analysis (FEA) has been done using ANSYS software to simulate computer models of structures for analyzing the strength. The boundary conditions are used as one fixed support and a 100N force applied to all structures. According to the analysis outcomes, this study intends to provide recommendations for designers about the different geometric shape strengths.

6.1 Yield strength

To perform the yield strength analysis, a CAD model has done in SolidWorks software and exported as STEP or IGES files, then imported to ANSYS. The material was selected as Polylactic acid (PLA). Fixed support and a force of 100N have been chosen for the boundary condition of model analysis. The boundary condition of the rectangular box model is shown in Figure 6.1. The fixed support is placed at the bottom and 100N pulling force at the top surface of the model.

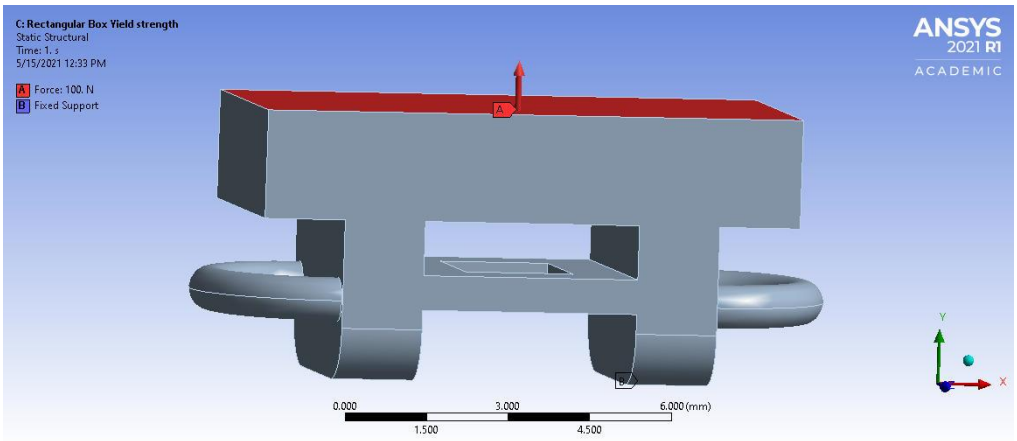

Figure 6. 1 The boundary condition of the rectangular box design.

This study explores the total deformation of the model using analysis. Figure 6.2 illustrates the maximum deformation .011 mm has been found at the middle of the top surface, and the value is significantly low.

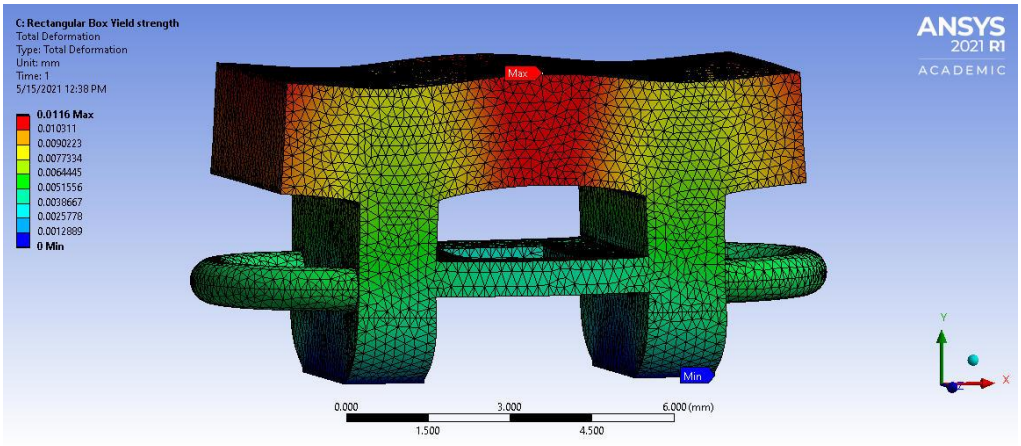

Figure 6. 2 The total deformation of the rectangular box design.

This study also examines the number of stress for the 100N tensile force. Figure 6.3, the maximum equivalent (von-Mises) stress has been obtained 36.2 MPa at the bottom of the model where the fixed support has been given.

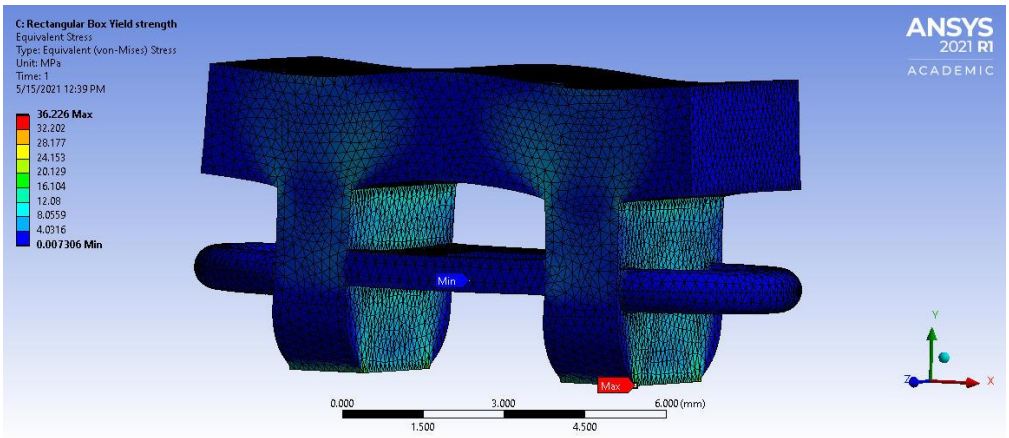

Figure 6. 3 The equivalent (von-Mises) stress of the rectangular model.

The same pulling force, 100N and fixed support at the bottom, has been applied to the modular model design (Figure 6.4). However, after running analysis, the deformation has been found 0.218 mm at both top-sided curved structures, which are unsupported in this model.

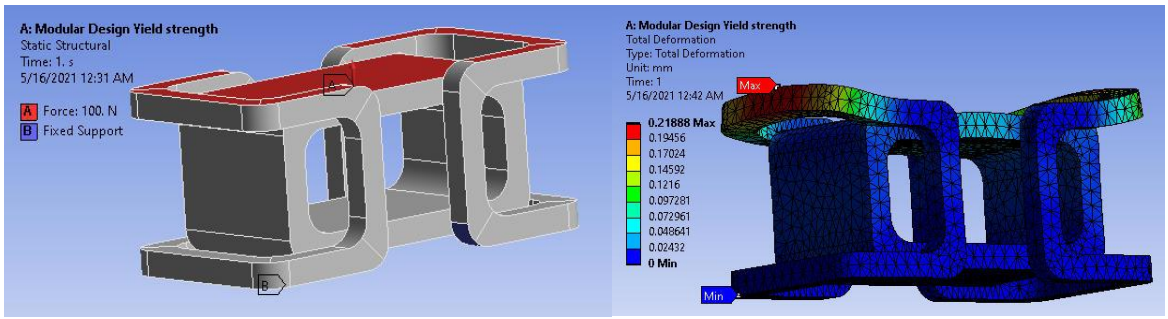

Figure 6. 4 The boundary condition (left) and the modular design's total deformation (right).

In the same analysis, the equivalent stress has been found 216.24 MPa at the connection between the curved shape and the rectangular body (Figure 6.5). At that point, the structure might start to create a fracture.

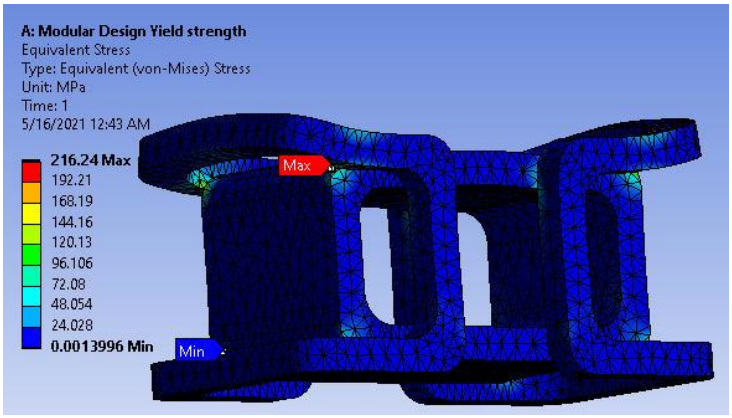

Figure 6. 5 The equivalent (von-Mises) stress of the modular design model.

The pentagon flat shape model has been fixed support at the bottom edge, and a pulling force of 100N has been applied at the top surface. As a result, the analyzed deformation has been found in the middle of the top surface of 0.075 mm (Figure 6.6)

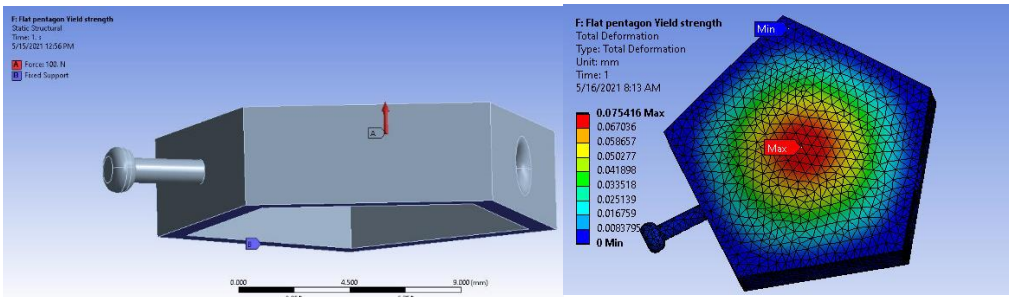

Figure 6. 6 The boundary condition (left) and the total deformation (right) of the pentagon flat design.

The region of concentrating the highest stress has been found at the hole part area. The equivalent stress of 24.19 MPa means that the crack might happen (Figure 6.7).

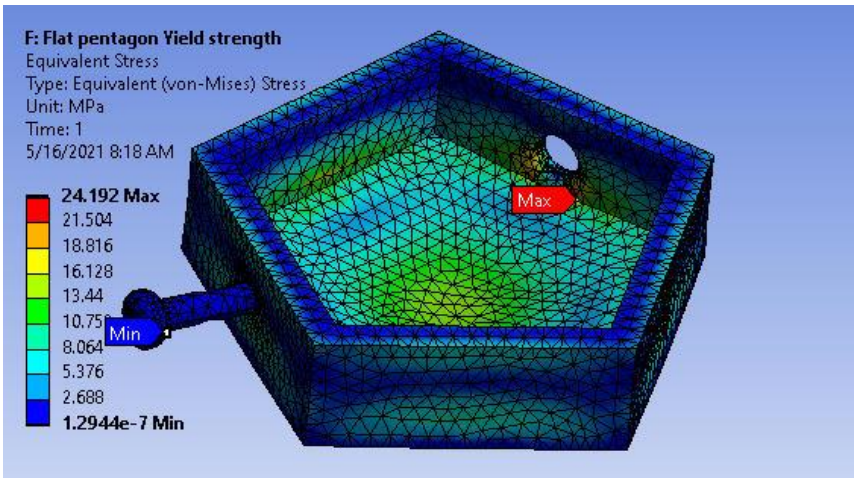

Figure 6. 7 The equivalent (von-Mises) stress of the pentagon flat design model.

For the pentagonal box shape model, the fixed support has been selected at the bottom of the model, and a 100N force has been applied at a pentagon area (edge 2.92mm) upward. As a result, the highest deformation, 1.24 mm, has been seen at the peak of the model (Figure 6.8).

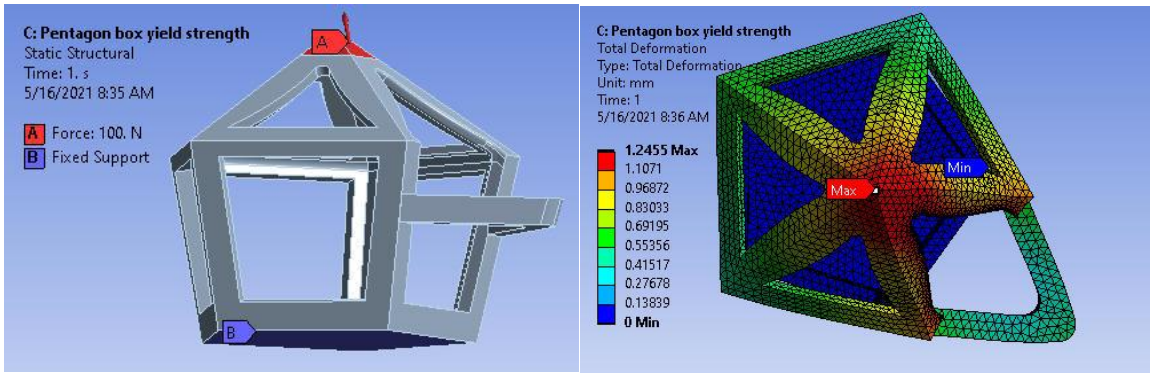

Figure 6. 8 The boundary condition (left) and the total deformation (right) of the pentagonal box design.

The equivalent stress in design has been found at the corner where the top inclined surface met with vertical side edges. Again, the stress is relatively high, 391.98 MPa at that point, illustrates in Figure 6.9.

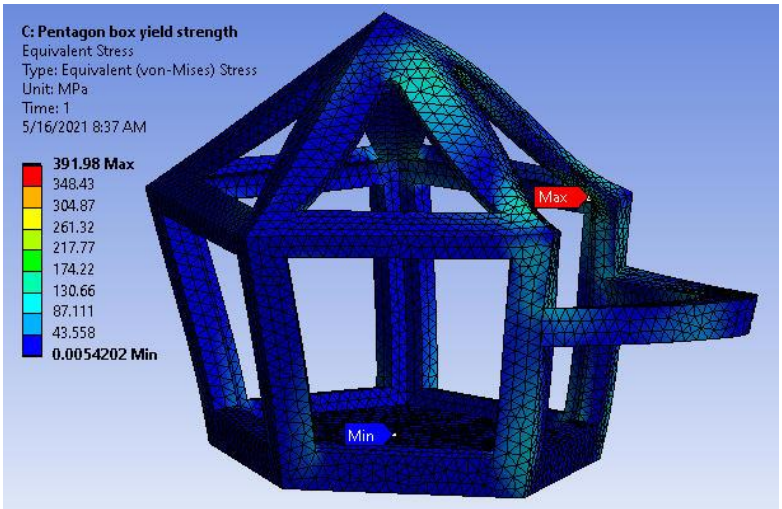

Figure 6. 9 The equivalent (von-Mises) stress of the pentagonal box design model.

In lantern design, the fixed support has been set up at the bottom faces, and a pulling force of 100N has been applied at the top sphere part (Figure 6.10). The analysis has been shown that the maximum deformation found at the inner face of the twisted surface, 0.228 mm.

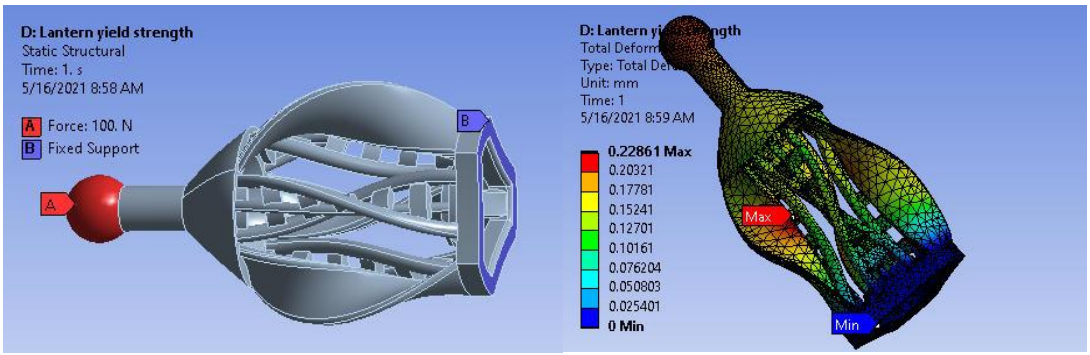

Figure 6. 10 The boundary condition (left) and the total deformation (right) of the lantern design.

The maximum concentrated stress has been formed at the connection point of the helix part with the upper conical shape. Therefore, the equivalent stress number is 130.53 MPa, separate from the body parts (Figure 6.11).

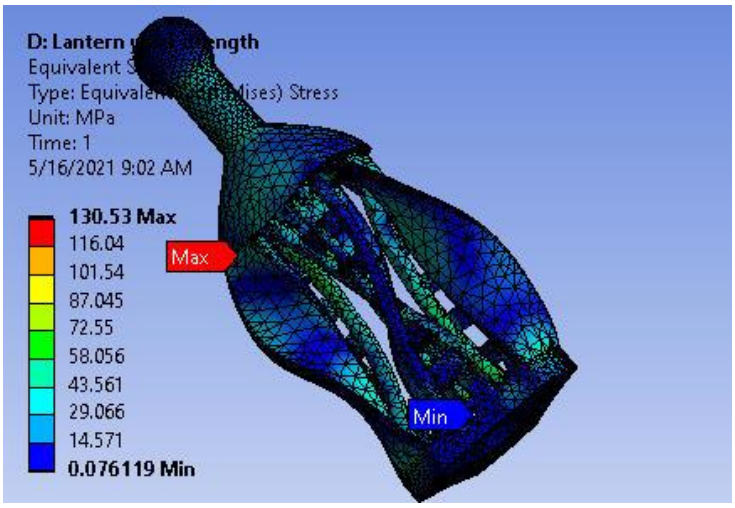

Figure 6. 11 The equivalent (von-Mises) stress of the lantern design model.

Table 6. 1 Summary of total deformation and equivalent stress of pulling force.

		Concepts									
		Rectangular shape		Modular design		Pentagon flat shape		Pentagonal box shape		Lantern shape	
Pulling force, 100 N	Units	Result	%	Result	%	Result	%	Result	%	Result	%
Total deformation	mm	**0.012**		0.219		0.075		1.246		0.229	
Equivalent stress	MPa	36.226	50 %	216.24	794 %	**24.192**	0 %	391.98	1520 %	130.53	440 %

From the above Table, 6.1 has observed that among the five models, the lowest deformation (0.012 mm) occurred in the rectangular shape model, and the lowest stress (24.192 MPa) was formed in the pentagonal flat shape model. Therefore, the design and manufacturing of the rectangular shape and pentagon flat shape model can be performed a satisfactory result. A complex geometric shape as lantern design could be chosen for the designer with more structural strength at the twisted and the helix shape during the design phase. However, the equivalent stress around 440% compared to the pentagonal flat design. The modular design yield stress is about 794% compared to the lowest stress. The pentagonal box design has been the highest value of deformation

and stress, which indicates that designing an inclined surface model needs to be more design optimization to reduce the stress.

6.2 Compressive strength

A similar method of study has been performed to analyze the effect of compressive force on the models. Instead of pulling force, a 100N compressive force has been applied among all models against fixed support. The total deformation and the equivalent stress have been recorded to compare and analyze for the design recommendations.

The rectangular shape design compressive boundary conditions and deformation are shown in Figure 6.12. The maximum deformation value has been found at the middle part of the top surface is around 0.0116 mm.

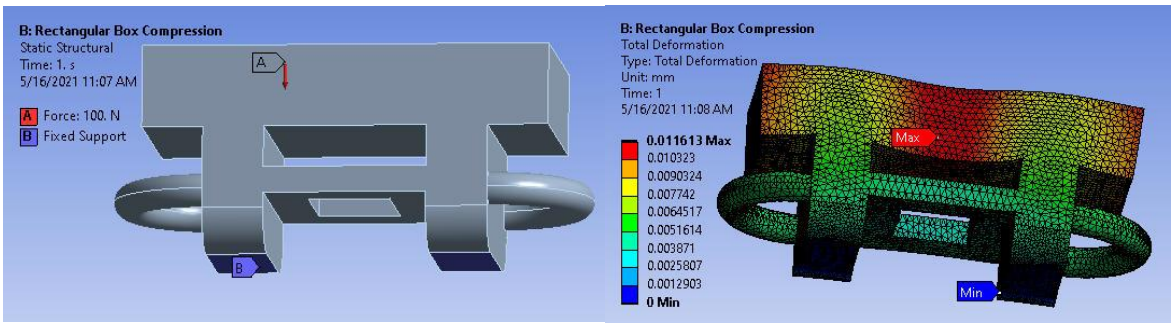

Figure 6. 12 The compressive boundary condition (left) and the total deformation (right) of the rectangular shape design.

The maximum equivalent stress of 42.51 MPa has been found at the bottom fixed support area (Figure 6.13).

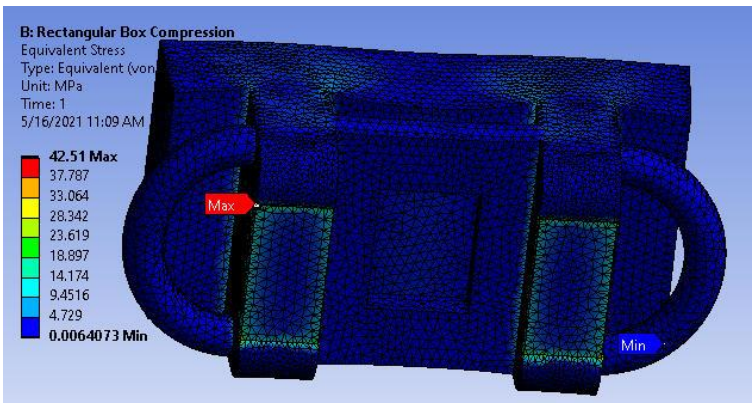

Figure 6. 13 The compressive equivalent (von-Mises) stress of the rectangular shape design.

A 100N compressive force has been applied in modular design on the upper surface area, and the fixed support has been employed at the bottom surface area. Figure 6.14 illustrates that the maximum deformation is 0.218 mm at the side edge of the design.

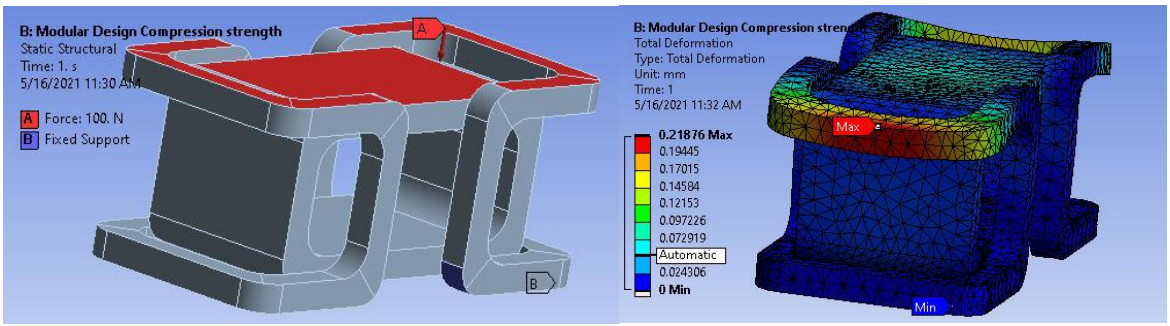

Figure 6. 14 The compressive boundary condition (left) and the modular design's total deformation (right).

The maximum stress of 176.35 MPa has been concentred in the joint of the elongate bar and rectangular bodies (Figure 6.15).

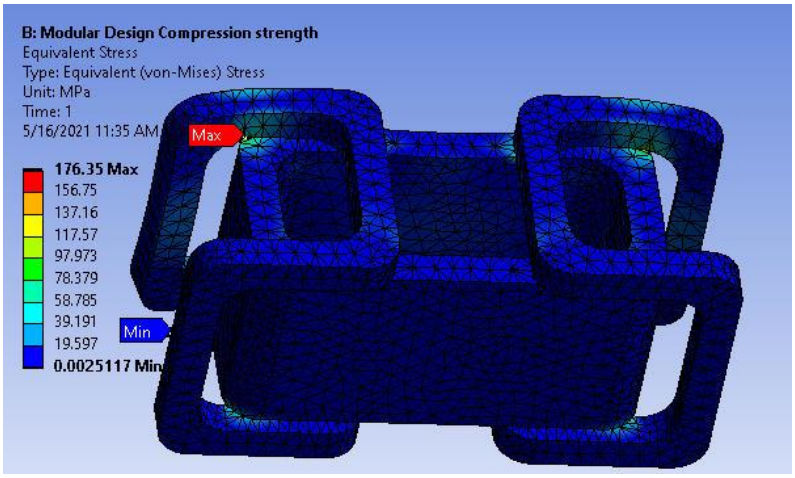

Figure 6. 15 The compressive equivalent (von-Mises) stress of the modular design.

The pentagon flat shape design has been examined with the same compressive force at the top surface and fixed support at the bottom part. As a result, in Figure 6.16, the maximum deformation of 0.075 mm has been found at the middle of the top surface.

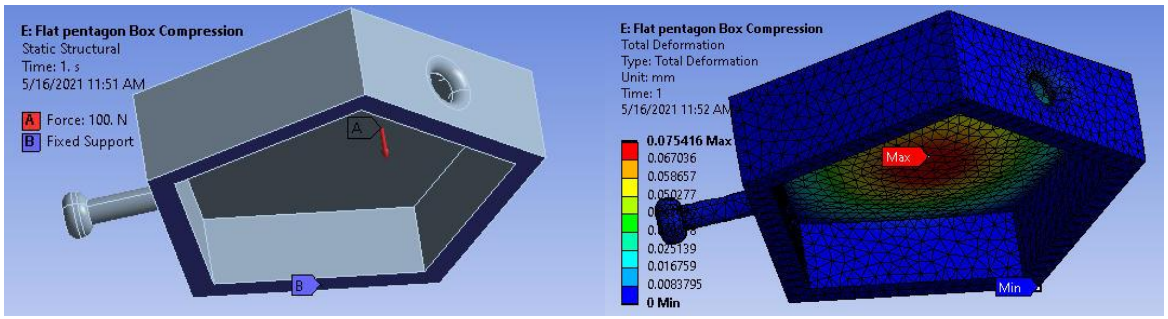

Figure 6. 16 The compressive boundary condition (left) and the total deformation (right) of the pentagon flat shape design.

The maximum stress has been found at the surrounding region of the hole area, and the stress is 24.19 MPa (Figure 6.17).

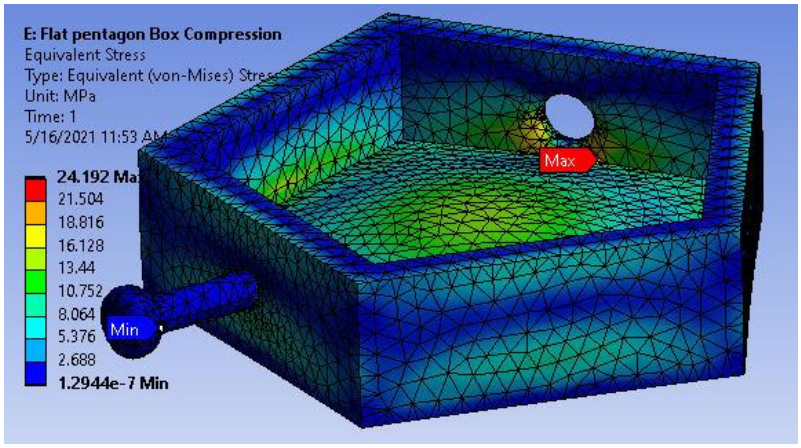

Figure 6. 17 The compressive equivalent (von-Mises) stress of the pentagon flat shape design.

A compressive force has been applied in a pentagonal box shape design with the same boundary conditions instead of pulling force. Figure 6.18 illustrates that the maximum deformation has occurred at the meeting point of the upper and side boundary edges.

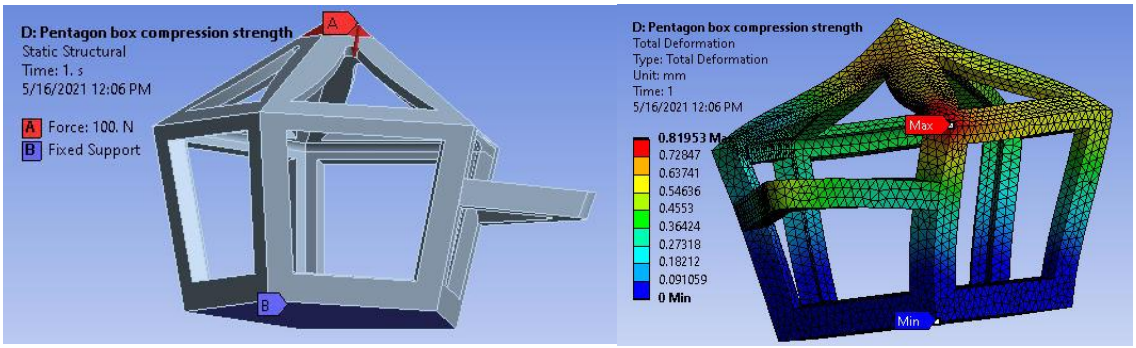

Figure 6. 18 The compressive boundary condition (left) and the total deformation (right) of the pentagonal box design.

Figure 6.19 shows that the maximum equivalent stress of 273.65 MPa has been found at the same point of the maximum deformation area. At that point, the model will break easily by a compressive force.

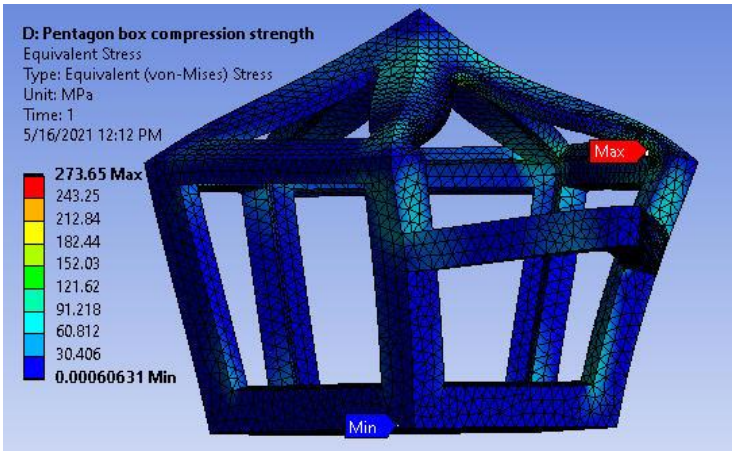

Figure 6. 19 The compressive equivalent (von-Mises) stress of the pentagonal box design.

The same compressive force has been applied to the lantern design, and the maximum deformation value has been found at the inner side of the twisted part. The value is 0.229 mm. Figure 6.20 illustrates that a compressive force could deform the comparatively weak geometric shape between the two base supports.

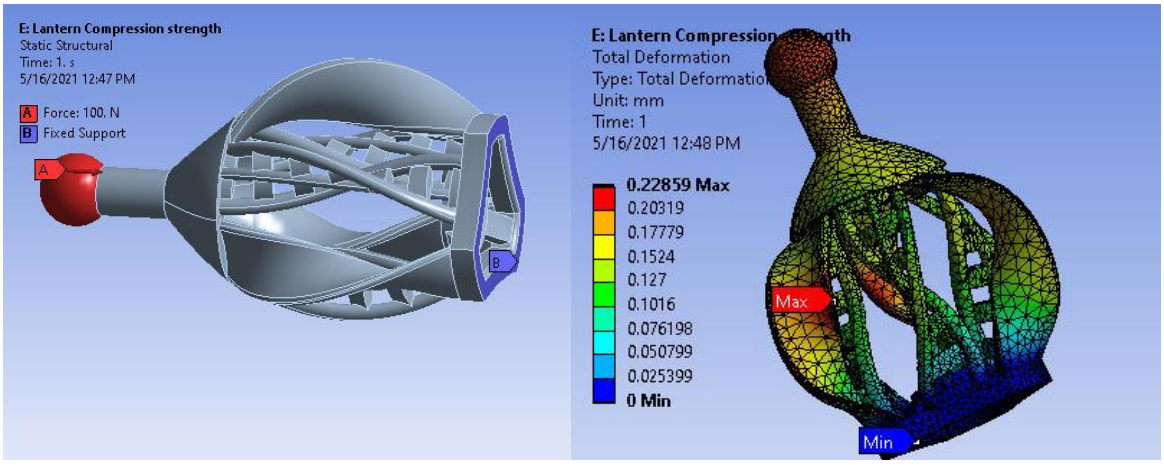

Figure 6. 20 The compressive boundary condition (left) and the lantern design's total deformation (right).

However, the maximum stress has been concentrated at the helix design (Figure 6.21). The weakest part of this structure has been found in twisted and helix design. This design could break earlier due to the compressive force applied.

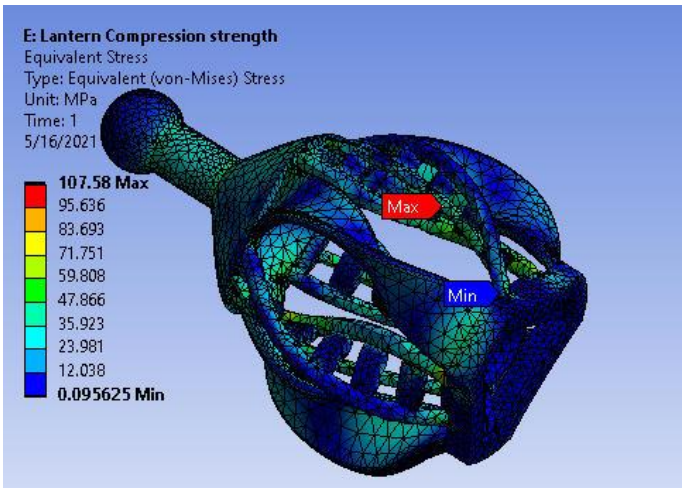

Figure 6. 21 The compressive equivalent (von-Mises) stress of the lantern design.

Table 6. 2 Summary of total deformation and equivalent stress of compressive force

		Concepts									
		Rectangular shape		Modular design		Pentagon flat shape		Pentagonal box shape		Lantern shape	
Compressive force, 100 N	Units	Result	%	Result	%	Result	%	Result	%	Result	%
Total deformation	mm	**0.012**		0.219		0.075		0.820		0.229	
Equivalent stress	MPa	42.51	76 %	176.35	629 %	**24.192**		273.65	1031 %	107.58	345 %

Table 6.2 shows that the pentagon flat design is the lowest value of stress and the lowest deformation is in the rectangular shape design. Both rectangular and pentagon flat design is manufacturable and less complexity of the design. The lantern design shows that it would be desirable to choose, though the twisted and helix part needs more durability strength. The modular design would be capable of resisting force if the overhanging side design could be modified to reduce stress. The pentagonal box design needs to optimize the corner intersecting point to reduce the high concentration of stress.

6.3 Critical situation analysis

Further analysis has been considered for the critical situation that could be happened in the real-life scenario. The severest case that could be happened when the user will use the designed jewelry. This study has explored at least one critical situation for each of the models. The applied magnitude of the force is the same as 100 N. By changing the boundary conditions, and this analysis observed the total deformation and equivalent stress of each model.

The boundary conditions for the rectangular shape design shown in Figure 6.22. The situation has been considered that the two half-circle rings pull up with 100N of force outward and the fixed support at the bottom of the model. As a result, the maximum deformation of 0.169 mm has been found in the middle of the ring.

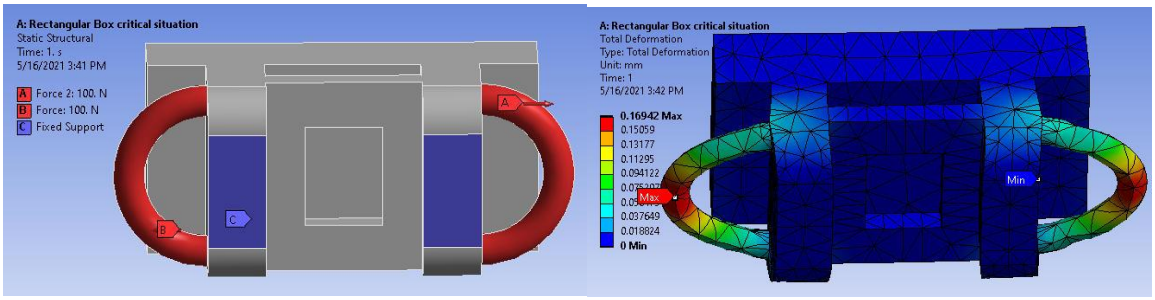

Figure 6. 22 The critical situation boundary condition (left) and the total deformation (right) of the rectangular shape design.

The maximum stress has been developed ring connector point to the body. The stress 239.37 MPa, assumes that the ring will disconnect from the body (Figure 6.23).

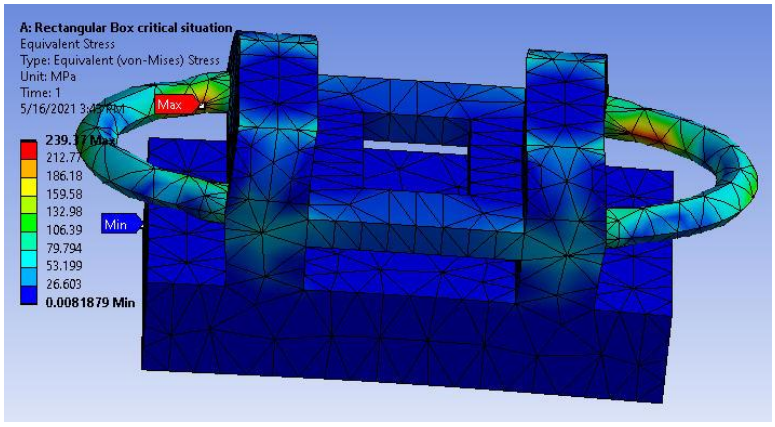

Figure 6. 23 The critical situation equivalent (von-Mises) stress of the rectangular shape design.

The modular design has been considered for a critical situation where two reverse 100N forces would apply at the inner face of the rectangular body and fixed support at the

bottom. That case could happen when the link finds a force from other links. As a result, the maximum deformation of 0.040 mm has found at the middle area of the inner face of the model, as shown in Figure 6.24.

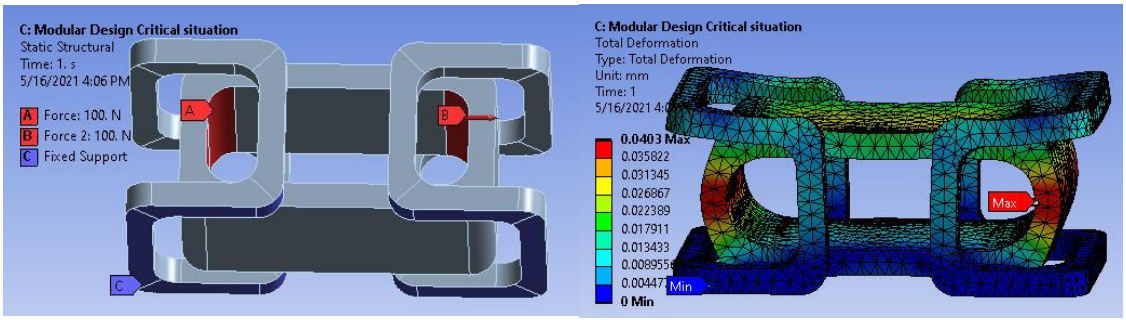

Figure 6. 24 The critical situation boundary condition (left) and the total deformation (right) of the modular design.

The maximum stress has been found at 66.48 MPa, the same point of compressive strength (Figure 6.25).

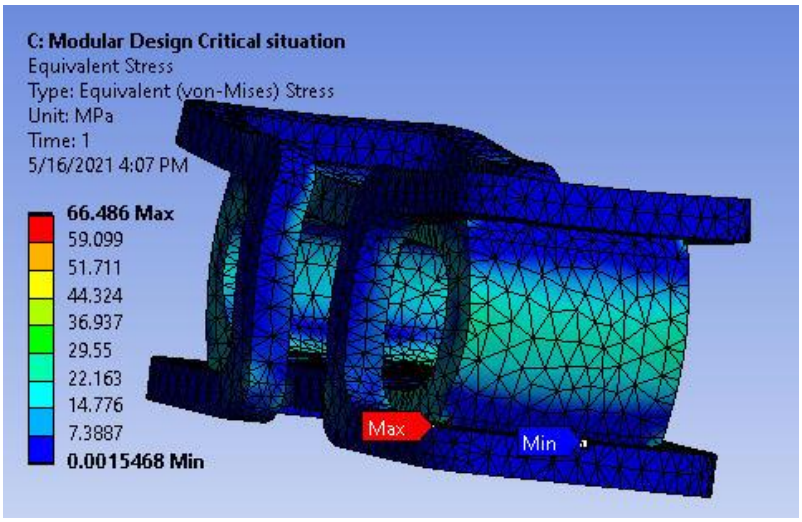

Figure 6. 25 The critical situation equivalent (von-Mises) stress of the modular design.

In the pentagon flat shape design, the spherical head connector is considered the fixed support and force applied to the top surface to simulate the model's moving conditions. As a result, the 22.27 mm deformation has been found at the edge corner of the model (Figure 6.26).

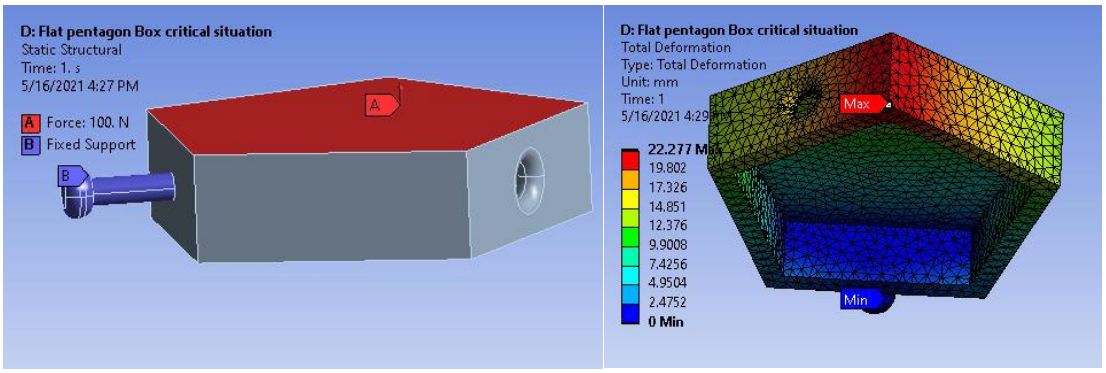

Figure 6. 26 The critical situation boundary condition (left) and the total deformation (right) of the pentagon flat design.

The maximum stress of 3152.3 MPa has been found at the joining point of the connector to the body.

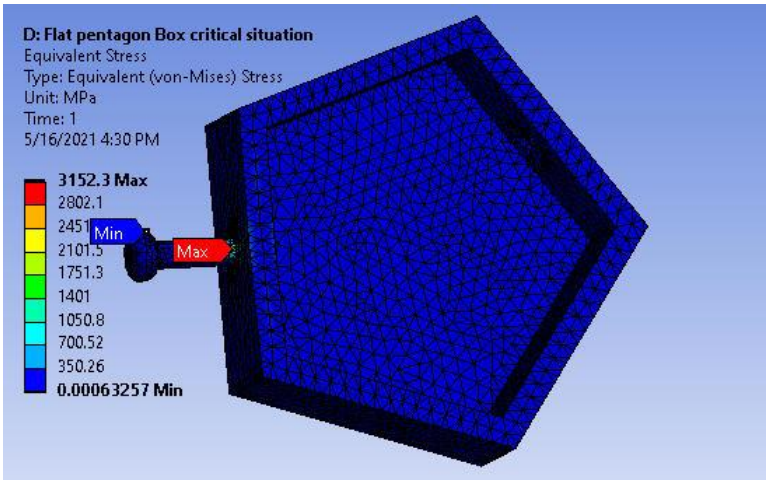

Figure 6. 27 The critical situation equivalent (von-Mises) stress of the pentagon flat design.

For the pentagonal box design, the critical situation has been considered when one link of design is pulled by the following link and how the interconnector will behave. As a result, a 100N force has been applied at the inner face of the connector, and the bottom part remained fixed. As a result, the maximum deformation of 1.4 mm has been found at the connector's peak (Figure 6.28).

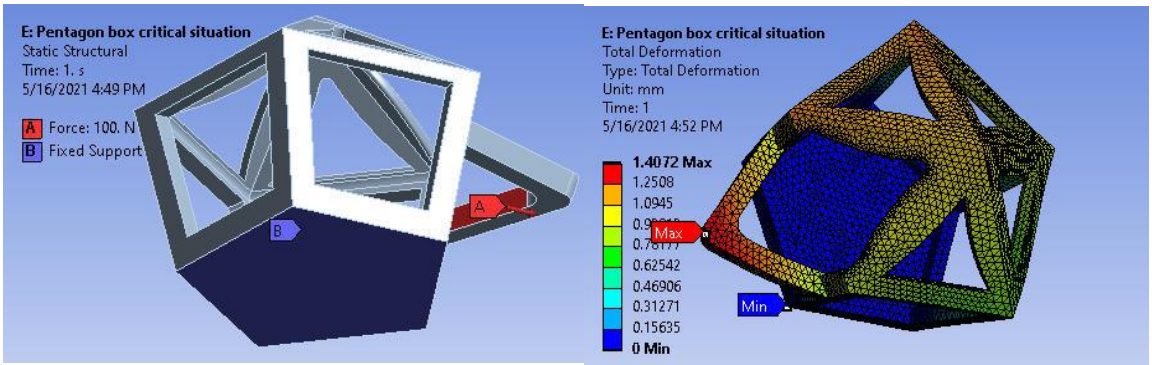

Figure 6. 28 The critical situation boundary condition (left) and the total deformation (right) of the pentagonal box design.

The maximum stress area has been found in the bottom leg inner corner, as shown in Figure 6.29. The pulling force would break the structure at this point.

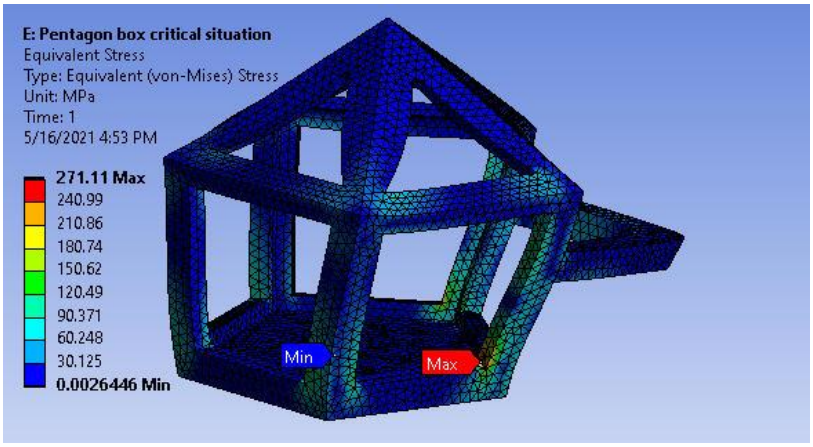

Figure 6. 29 The critical situation equivalent (von-Mises) stress of the pentagonal box design.

The lantern design's critical situation has been considered when a user wears it, and an external force could be hit on the edge of a twisted or helix design. The other side of the lantern would be supported on the skin. Therefore, fixed support and 100N of force have been applied to the lantern body, as illustrated in Figure 6.30. The maximum deformation of 1.12 mm has been found at the top edge of the twisted part.

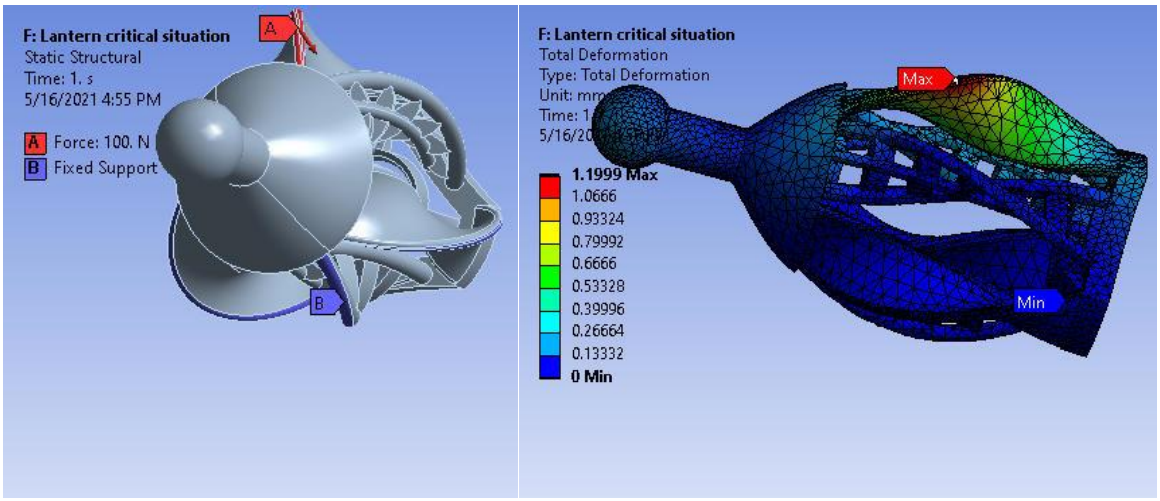

Figure 6. 30 The critical situation boundary condition (left) and the total deformation (right) of the lantern design.

Figure 6.31 illustrates that the maximum stress of 439.5 MPa has been found at the bottom connecting point of the twisted part to the base.

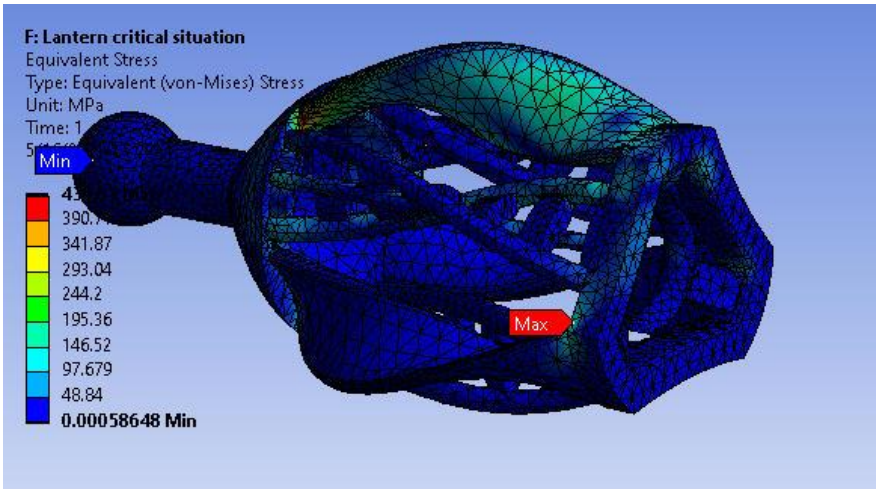

Figure 6. 31 The critical situation equivalent (von-Mises) stress of the lantern design.

As the finite element analyses for the all-designed model, the result has been found that the less complex shape models such as rectangular shape and pentagonal flat shape model have less equivalent stress than other models. The designers who want to develop a more robust model, these types of simple geometric shape model are more suitable for manufacturing. Preferring the complex geometric shape like the lantern design requires more geometrical shape analysis and stronger shape design for manufacturable jewelry. If the strength of the design is less critical for useability and the complex shape is desired, the designer could choose this type of shape. The result for modular design has been shown that the stress concentration is higher only at a specific point. So, if a designer could optimize the stress localized area, it would be a

flexible design for manufacturing in 3D printers. With modular design, there could be a wide range of possibilities to create a variety of designs. For example, the designer who wants to create jewelry with some space inside for setting up any free moving object could choose the pentagonal box type design. According to the analysis, if the maximum stress can be reduced by redesign or optimization, these designs could be preferable.

7. PHYSICAL TESTING

A physical tensile test has been done by a tensile testing machine, "Tinius Olsen H10KT"[48], in the laboratory (Figure 7.1). For tensile testing, four kinds of design specimen have been selected. The specimens were designed to grip in a test machine gripper. The test specimens were printed in both XY-axis and Z-axis printing orientations. The test specimen was positioned vertically, two gripped vice, and pulled at a predetermined load range. When it reached the breaking force, then the test was stopped. The graphical representation of the test result was recorded.

Figure 7. 1 Tinius Olsen tensile testing machine.

7.1 Pentagonal box specimen test

The test specimen has been printed in both XY and Z directions of printing. A total of six specimens was tested in 100N of load range and 1 mm/min speed. The test was continued until the fracture occurred. Figure 7.2 illustrates the specimens after the test.

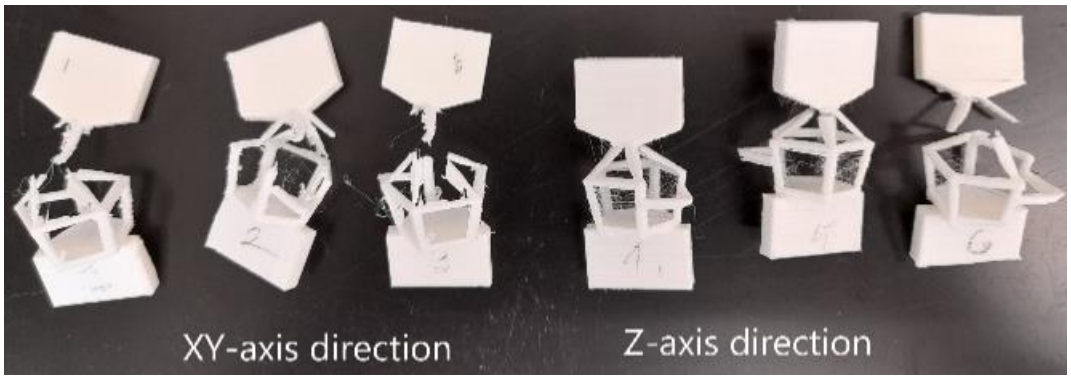

Figure 7. 2 Pentagonal box specimen after the test.

Analysis of Graph: A graphical representation of force(N) and extension(mm) is shown in Figure 7.3. In this graph, three (1-3) specimens were printed in the XY-direction and the last three (4-6) in the Z-direction.

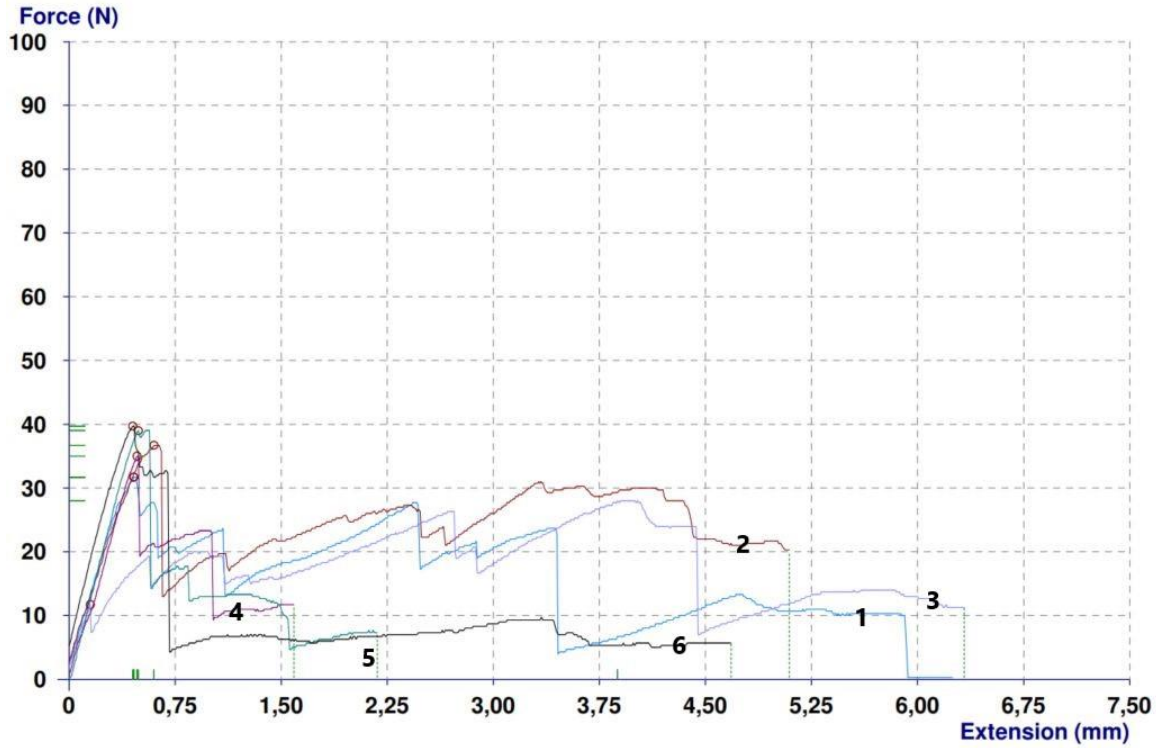

Figure 7. 3 Force and extension graph for pentagon box specimen.

The maximum yield force (39.7 N) was found in the Z-direction test specimen. However, the maximum extension was found in the XY-direction test specimen. The yield force for all specimen found a closer value. Specimen 1 and 2 first broke almost at the same force, and the elongation was similar. Though specimen 3 broke at little force, and the extension was the highest. Z-direction printed specimen broke at high yield force, but the extension was found less than the first three specimens. XY-direction of printing

indicated the more prolonged elongation because the printing filament elongates in the pulling force direction. In contrast, the Z-direction specimens showed less elongation due to the layer of the printing. The test result is included in appendix 1.

Analysis of test result: The tensile test result of the pentagonal box are tabulated in Table 7.1.

Table 7. 1 Tensile test result for pentagonal box

Pentagonal Box						
Specimen no. and orientation of printing		Yield Force (N)	Force at break (N)	Area(mm^2)	Yield Stress (MPa)	Stress at break (MPa)
XY direction	1	31.7	0.3	16.59	1.91	0.02
	2	36.7	20.3	16.59	2.21	1.22
	3	11.7	11.3	16.59	0.71	0.68
Z direction	4	35	11.7	16.59	2.11	0.71
	5	39	7.3	16.59	2.35	0.44
	6	39.7	5.7	16.59	2.39	0.34

The yield force value obtained for XY orientation shows a very close value except specimen 3. The breaking points of all specimens showed that the most stress concentration region is similar to the ANSYS analysis. The first specimen was broken at a first point in the top surface, and then it elongates again until the next break. In that phase, the force decreased gradually, and the elongation was long because the tensile force pulled in the same direction as the printing filament. Though the fracture occurred at maximum yield force, the plastic deformation tends to be more elongated. The Z-axis orientation specimens fractured at yield force as similar to the specimen 1 and 2; however, the elongation was less in comparison.

The most stress-generating region has been found as the strength analysis in ANSYS. The comparatively higher yield stress is found in Z-direction specimens. However, the stress at break is lower than in XY-direction specimens. The fracture point of test specimens confirms that the ANSYS calculation is acceptable. In the physical test specimen, the maximum stress has found 2.39 MPa whereas, in ANSYS analysis, 392 MPa. The lowest yield stress was found at 0.71 MPa in specimen 3 at the lowest yield force of 11.7 N.

7.2 Lantern specimen test

The three test specimen has been printed in XY-axis and three in Z-axis directions of printing. Thus, six specimens were tested in 1000N of load range and 1 mm/min speed. The test was continued until the fracture occurred. Figure 7.4 illustrates the specimens after the test.

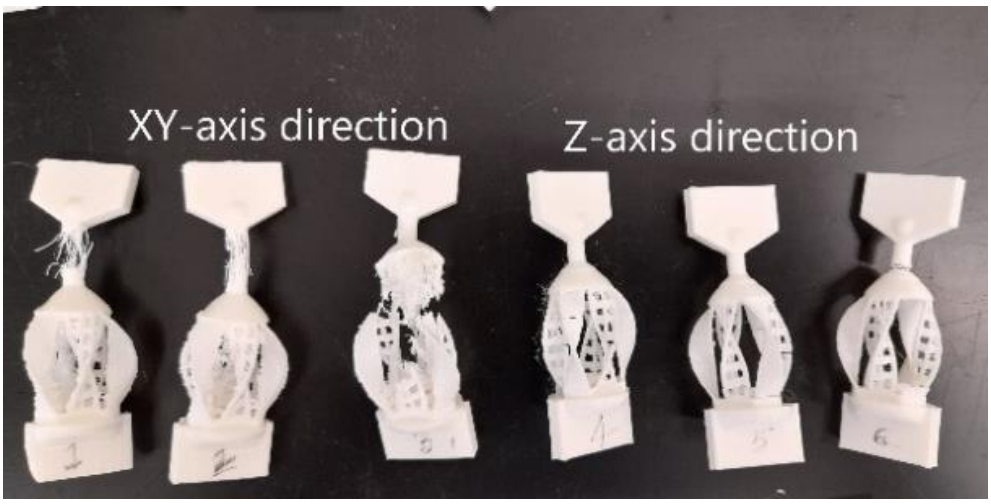

Figure 7. 4 Lantern specimen after the test.

Analysis of Graph: A graphical representation of force(N) and extension(mm) is shown in Figure 7.5. In this graph, three (1-3) specimens were printed in the XY-direction and the last three (4-6) in the Z-direction.

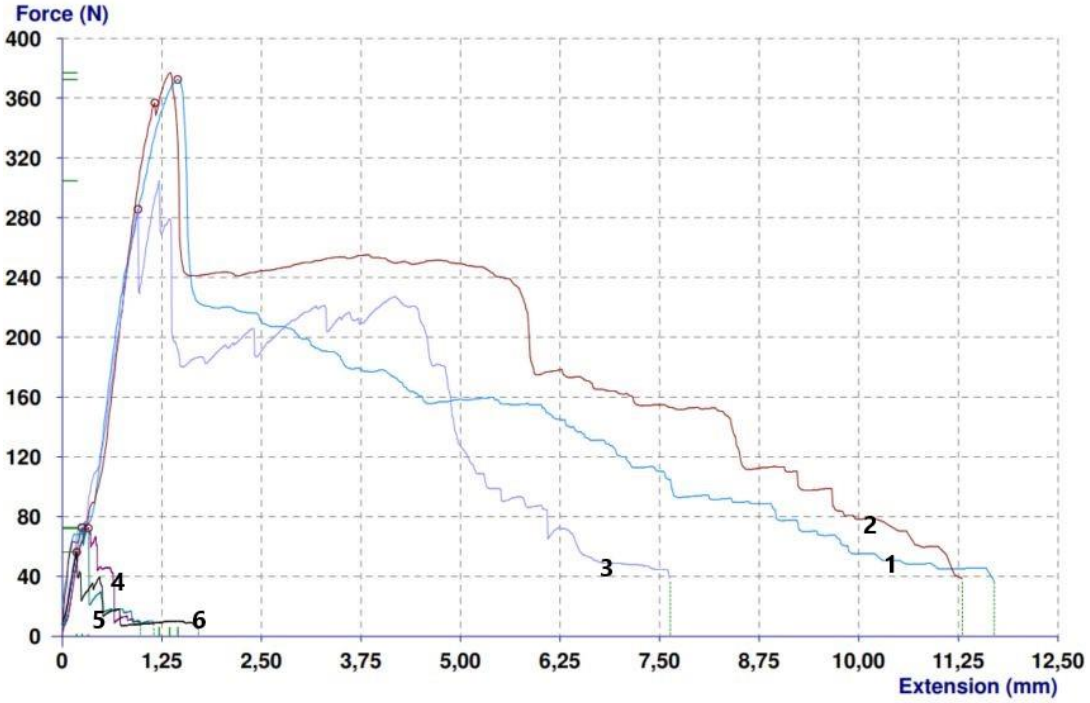

Figure 7. 5 Force and extension graph for lantern specimen

The maximum yield force (372.4 N) was found in the XY-direction test specimen, and the minimum value was 56.3 N in the Z-direction specimen, which is almost 561% lower. Moreover, the maximum extension was found in the XY-direction test specimen. The yield force value in the XY-direction and Z-direction specimens found substantial differences. Specimen 1 and 2 first broke almost the same force, and the elongation was similar. Though specimen 3 broke at a smaller force. Z-direction printed specimen broke at a lower yield force and with lower extension compared to XY-direction. XY-direction of printing indicated the more prolonged elongation because the printing filament stretches in a pulling force direction. In comparison, the Z-direction specimens showed less elongation due to the layer of the printing. The test finding is included in appendix 2.

Analysis of test result: The tensile test result of the lantern specimen are tabulated in Table 7.2.

Table 7. 2 Tensile test result for the lantern

Lantern						
Specimen no. and orientation of printing		Yield Force (N)	Force at break	Area(mm^2)	Yield Stress (MPa)	Stress at break (MPa)
XY direction	1	372.4	36.8	12.57	29.63	2.93
	2	356.8	38.4	12.57	28.39	1.26
	3	285.6	38.8	30.52	9.36	1.27
Z direction	4	72.3	9.69	30.52	2.37	0.32
	5	72.7	7.3	30.52	2.38	0.24
	6	56.3	5.7	12.57	4.48	0.45

The yield force value found for XY orientation shows a closer value except specimen 3. The breaking points of specimens 1 and 2 showed that the most stress concentration region of the cylindrical shape of the lantern. The cylindrical shape was hollow inside. As the infill rate was not 100%, that made the stress concentration in this part. However, the rest of the specimen's fractured region was similar to the ANSYS analysis. The first two specimens were broken at the cylindrical shape in the top surface, and then it elongated again until the complete separation. Since the tensile force pulled the printing material, the force gradually decreased, and the extension was long during that process. On the other hand, specimens 4,5,6 broke at the twisted surface and helix shape at the maximum yield force, separated without much elongation.

The most stress-generating region has been found as the strength analysis in ANSYS. The comparatively higher yield stress is found in XY-direction specimens. The stress at break is found higher than in Z-direction specimens. The fracture point of test specimens confirms that the ANSYS calculation is acceptable. Twisted and helix shapes are found as the weakest part of the lantern design. In physical test specimens, the maximum stress has found 29.63 MPa whereas, in ANSYS analysis, 130.53 MPa. The lowest yield stress was found at 2.37 MPa in specimen 4.

7.3 Helix specimen test

A separate helix shape specimen has been printed in XY-axis and Z-axis directions. Six specimens were tested in 1000N of load range and 1 mm/min speed. The test was continued until the fracture occurred. Figure 7.6 illustrates the specimens after the test result.

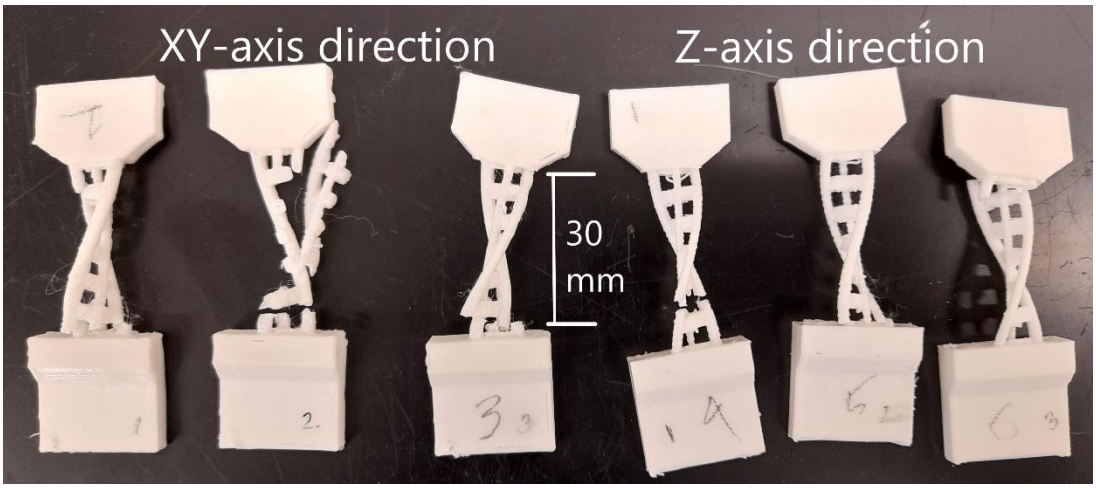

Figure 7. 6 Helix specimen after the test.

Analysis of Graph: A graphical representation of force(N) and extension(mm) is shown in Figure 7.7. In this graph, three (1-3) specimens were printed in XY-direction and the last three (4-6) in the Z-direction.

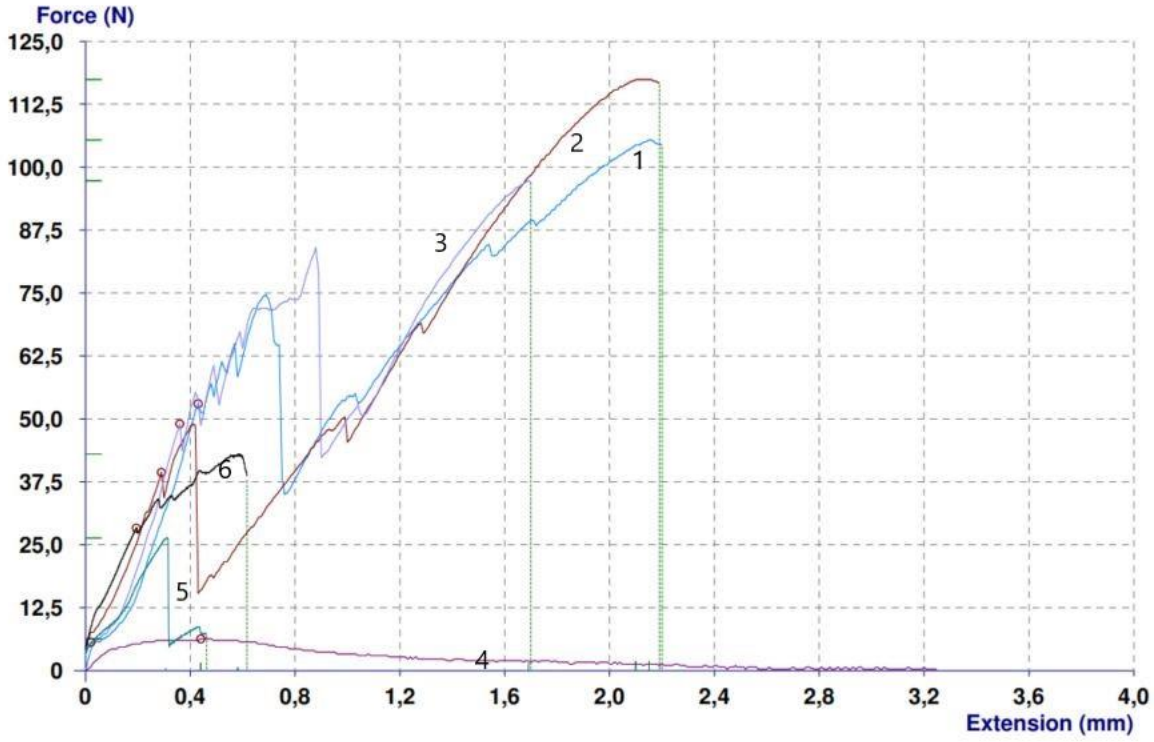

Figure 7. 7 Force and extension graph for helix specimen.

The maximum yield force (53.0 N) was found in the XY-direction test specimen, and the minimum force (5.66 N) was found in the Z-direction specimen, which is almost 836% lower. Moreover, the maximum extension was found in specimens 1 and 2 at the XY

direction. The first three specimens broke almost the same force, and the elongation was similar. Though specimen 5 broke at the lowest force (5.66 N). Z-direction printed specimen broke at a lower yield force and with small extension compared to XY-direction. XY-direction of printing indicated the more prolonged elongation because the printing filament stretches toward the pulling force direction. Whereas the Z- direction specimens showed less elongation due to the layer of the printing. The fracture occurred between the layer of printed specimens. The test result is in appendix 3.

Analysis of test result: The tensile test result of the lantern specimen are tabulated in Table 7.3.

Table 7. 3 Tensile test result for the helix shape

Helix						
Specimen no. and orientation of printing		Yield Force (N)	Force at break	Area(mm^2)	Yield Stress (MPa)	Stress at break (MPa)
XY direction	1	53	104.4	8.28	6.40	12.61
	2	39.38	116.6	8.28	4.76	14.08
	3	49	97	8.28	5.92	11.71
Z direction	4	6.3	0.3	8.28	0.76	0.04
	5	5.66	7.3	8.28	0.68	0.88
	6	28.34	38.7	8.28	3.42	4.67

The yield force value found for XY orientation shows a similar range of values. The breaking points of specimens 1,2 and 3 showed that the most stress concentration region of the cylindrical shape of the helix. The rest of the specimen's fractured region was similar to the ANSYS analysis. The first two specimens were broken at the larger surface areas of the cylindrical shape. Then it elongated again until the complete separation. In that phase, the force increased gradually, and the elongation was long because the tensile force pulled in the same direction as the printing filament. On the other hand, specimens 4,5,6 broke between the layer of cylindrical shape at the minimum yield force, separated without much elongation.

The most stress-generating region has been found similar to the strength analysis in ANSYS. The comparatively higher yield stress and the stress at break are found in XY-direction specimens. The fracture point in test specimens confirms that the ANSYS calculation is acceptable. The weakest part of the helix is found in twisted cylindrical shapes. In the physical test specimen, the maximum stress has found at 6.40 MPa. The lowest yield stress was found at 0.68 MPa in specimen 5.

7.4 Twisted shape specimen test

A separate helix shape specimen has been printed in XY-axis and three in Z-axis directions of printing. Specimens were tested in 100N of load range and 5 mm/min speed. The test was continued until the fracture occurred. It was the first experiment in this test. Two specimens were broken due to an inappropriate machine setup. Therefore, three specimens in XY-direction and one specimen in Z-direction have been tasted. Figure 7.8 illustrates the specimens after the test.

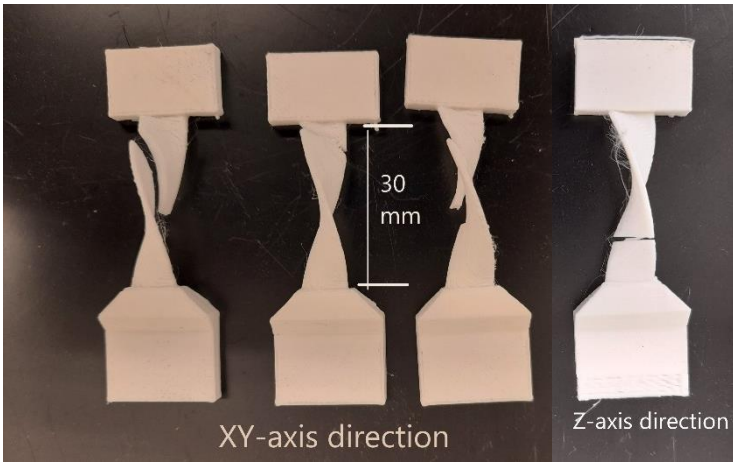

Figure 7. 8 Twisted shape specimen after the test.

Analysis of Graph: A graphical representation of force(N) and extension(mm) is shown in Figure 7.9. In this graph, specimen 1,4,5 was printed in the XY-direction, and specimen 3 in the Z-direction.

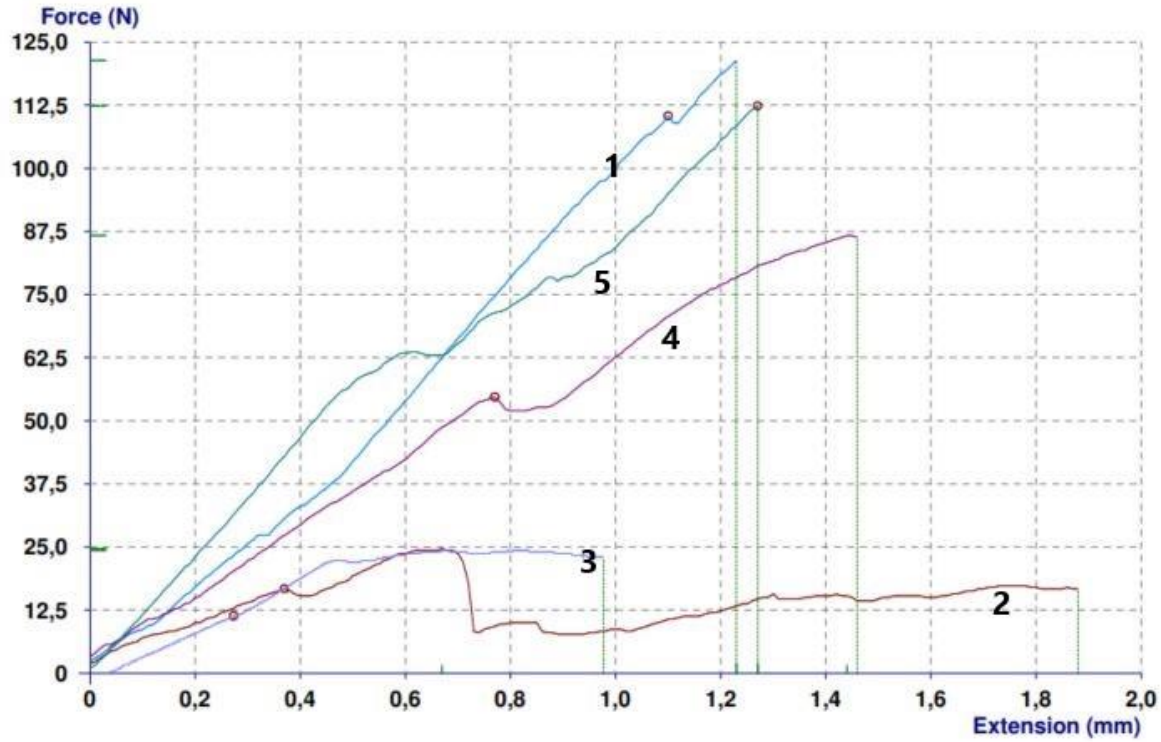

Figure 7. 9 Force and extension graph for twisted shape specimen.

The maximum yield force (112.4 N) was found in the XY-direction test specimen, and the minimum force (11.3 N) was found in the Z-direction specimen, which is almost 894% lower. Moreover, the maximum extension was found in the XY direction specimens. The first three specimens broke almost the same force, and the elongation was similar. Specimen 3 broke at the lowest force. Z-direction printed specimen broke at a lower yield force and with small extension compared to XY-direction. The test result is in appendix 4.

Analysis of test result: The tensile test result of the lantern specimen are presented in Table 7.4.

Table 7. 4 Tensile test result for the twisted shape

Twisted shape						
Specimen no. and orientation of printing		Yield Force (N)	Force at break	Area(mm^2)	Yield Stress (MPa)	Stress at break (MPa)
XY direction	1	110.4	121.4	12.16	9.08	9.98
	4	54.7	86.7	12.16	4.50	7.13
	5	112.4	112.4	12.16	9.24	9.24
Z direction	3	11.3	23	12.16	0.93	1.89

The yield force value found for XY orientation shows different values. The specimens 1 and 5, the yield force was closer. However, specimen 4 force was almost half. The breaking points of all XY-direction specimens were found similar. The specimens were broken at the larger surface areas of the twisted surface. Before the breaking point, it elongated towards the force direction. In that phase, the force increased gradually. On the other hand, specimen 3 broke between the layer of cylindrical shape at the minimum yield force. In this experiment, specimen 2 does not show the actual result because of a manufacturing defect.

The most stress-generating region has been found similar to the strength analysis in ANSYS. The comparatively higher yield stress is found in XY-direction specimens. The fracture point in test specimens confirms that the ANSYS calculation is acceptable. The weakest part of the helix is found in twisted surface shapes. In the physical test specimen, the maximum stress has found at 9.24 MPa. The lowest yield stress was found at 0.98 MPa in specimen 3.

According to the physical tensile test analysis, a significant tensile strength has been found in the XY-axis direction printing rather than the Z-axis direction. The experiment shows the sufficient yield stress difference in printing orientation for all test specimens except the pentagonal box. The ANSYS analysis and tensile test results have found similar behavior during the experiment. The specimen printed in XY orientation has been found greater tensile strength than the Z orientation specimen. Therefore, designers aiming to print jewelry by desktop 3D printers need to be aware of this printing orientation during the designing and printing phase. If the design required tensile strength, it is recommended to choose the XY printing direction with a design like a lantern, pentagonal box. Therefore, this study observed that a critical geometric shape as twisted shape, helix shape visual quality was not satisfactory in XY-direction printing. Thus, if the printing quality is required for the designer, then they can choose Z orientation printing. However, the desired yield strength might be lower. Consequently, according to the objective and idea, a designer can incorporate these study results during the design and manufacturing of jewelry.

8. LED JEWELRY

3D printed LED (light-emitting diodes) jewelry is becoming popular in recent times. This study has been investigated to include LED components with the pentagonal box design. Small construction mountable SMD (surface mounted device) LED has been considered for this design which can be mounted inside the box. A watch battery or coin battery, a small switch, and SMD LED were chosen for design (figure 8.1).

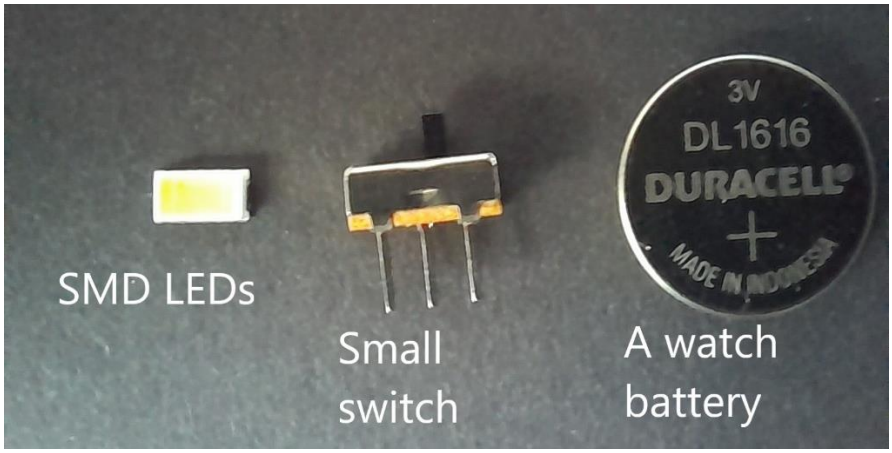

Figure 8. 1 Illustration of SMD LEDs, Small switch, and watch battery.

The design of the pentagonal box has been redesigned to set up the LEDs. In addition, a battery and a small switch holder are designed for the energy source (figure 8.2).

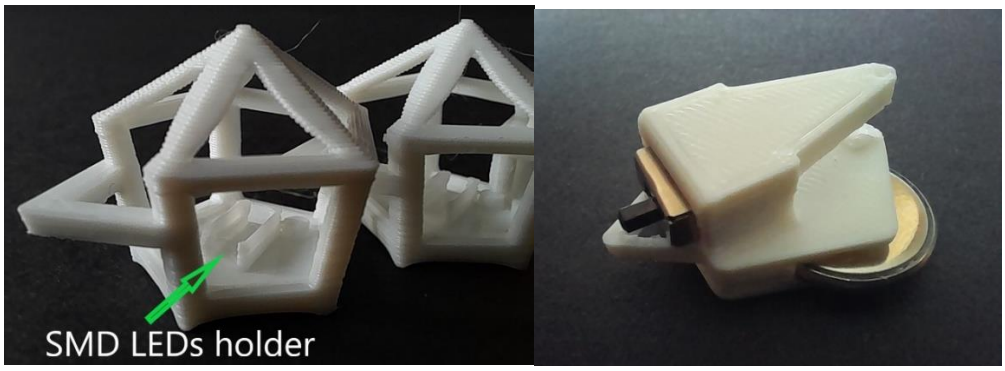

Figure 8. 2 Pentagonal box with LED holder (left); a battery and switch holder (right)

A circuit has been designed for LED jewelry. The SMD LEDs are connected in parallel, and the battery, resistor in a series connection with wire. The circuit is shown in Figure 8.3.

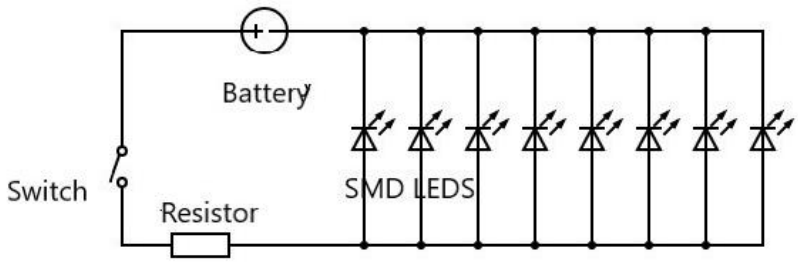

Figure 8. 3 A circuit design.

The circuit was completed with a connector wire soldering. The complete circuit was placed in the pentagonal box after the completion of LED holder parts. Figure 8.4 illustrates the manufacturing steps and after completion of printing.

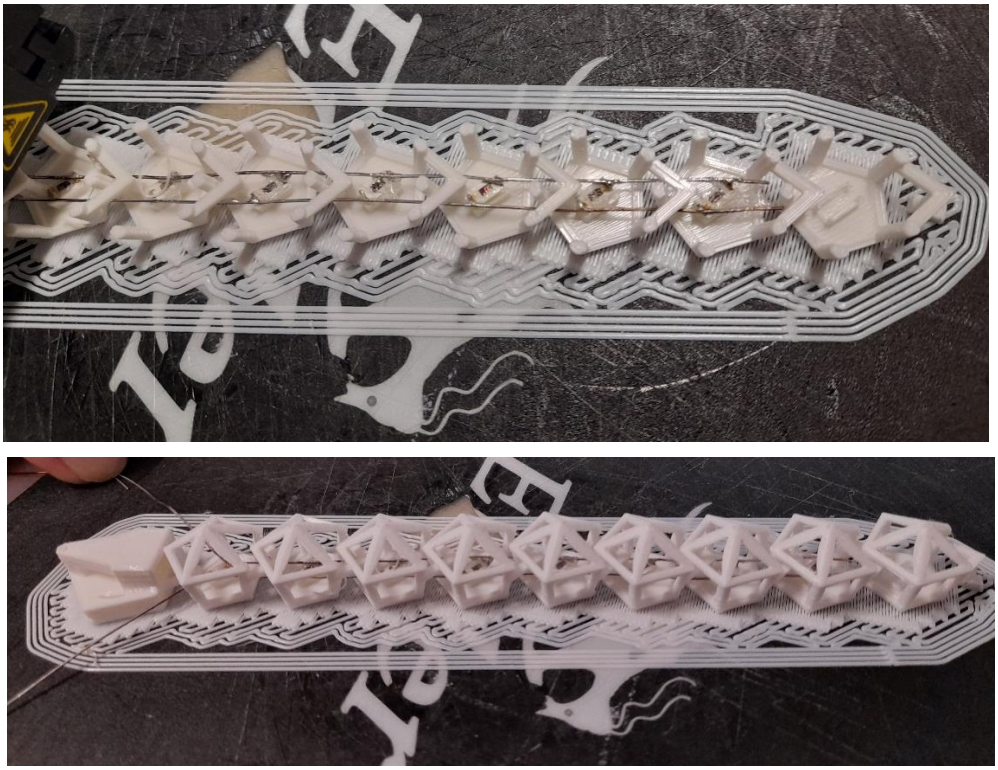

Figure 8. 4 The manufacturing steps of the pentagonal box with LED.

After printing, the box chain along with the battery holder was detached from the printing supports. Thus, the switch and the battery were placed into the battery holder. The outcome is shown in Figure 8.5.

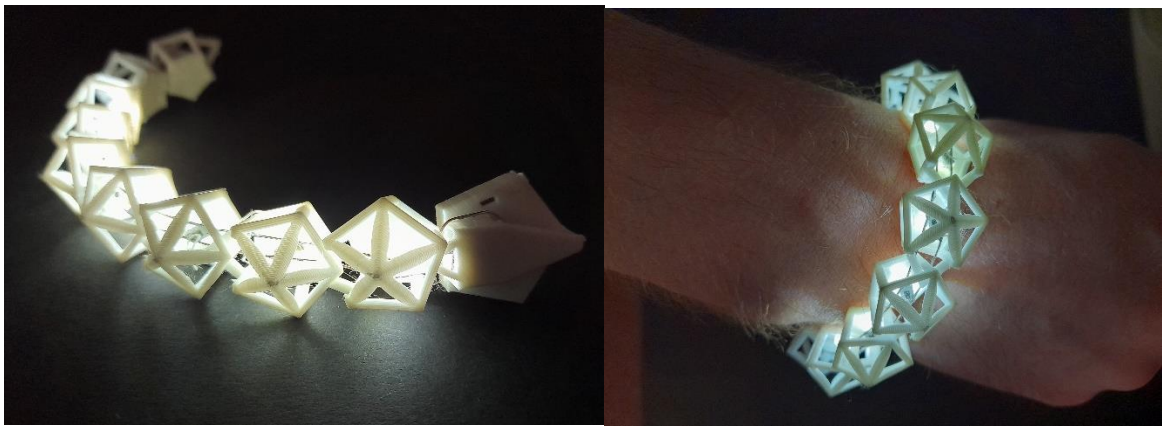

Figure 8. 5 The outcome of the pentagonal box bracelet with LED.

The observation from LED jewelry has been found that the flexibility was lost limited due to thicker wire. The LEDs were pulled off from the holder because of the inflexibility of the wire. Therefore, removing support from the battery holder also made the process much complicated. Furthermore, during the soldering process, it needed more concentration. Otherwise, the LED could be damaged easily. Therefore, the battery holder design needs to improve to make it more functional.

The recommendation for the designer could be about the selection of flexible connecting wire. The wire should have flexible enough that it could stretch and compress to an allowable limit. The idea of placing the circuit in between printing times was not good enough because the printer can create some errors. The length of printing in the XY axis direction also has the limitation of printed chain length. In printing, a bracelet shape might need a longer length. The length could be one crucial design factor to the designer during the design stage. Moreover, if one bracelet link might get affected in cleaning time, the whole chain would suffer. So, it is also possible to think about an alternative way for assembling all links. The soldering process made the process complicated as the place for it was small. The designer could choose a different version of LED strips that available in the market. The ease of replacing the battery is essential for the design. In bracelet design, the battery holder could think about a push-fit design for replacing smoothly. For the further design of the switch, a push-button switch can be considered. Therefore, the recommendation could take into consideration in the production of the LED jewelry.

SUMMARY

Additive Manufacturing (AM) is an effective and rapidly changing manufacturing technique that uses computer-aided design (CAD) to create parts layer by layer. It offers design flexibility as well as environmental and ecological benefits. AM can produce parts with exceptionally intricated and complex geometries with minimal post-processing, with the least material waste, and appliable to a wide range of materials such as plastics and metals. In AM methods, Fused deposition modeling (FDM) has emerged as one of the most promising and cost-effective techniques for forming free-form parts. Recently there has been expanding interest in 3D printing jewelry for some intricated and sophisticated design.

The purpose of these studies to explore the area of 3D printed jewelry design, investigate the manufacturability of complex geometric shapes and forms, and strength analysis. The study's objective is to explore the manufacturability and strength analysis of complex geometric shape jewelry design, strength analysis of designed jewelry, and general guidelines for jewelry design and manufacturing.

This study starts with designing a jewelry model with general conceptions of basic geometric shape design. Then, the three-dimensional drawing has been done with CAD software SolidWorks to visualize the design. Next, a desktop 3D printer has been used for printing the designed model with Polylactic acid (PLA) material. Next, for finite element analysis, ANSYS software has been used to investigate the tensile, compressive, and critical situation analysis. Finally, a physical tensile test has been performed for the 3D printed model by a universal testing machine.

As the finite element analyses for the designed model, the result has been found that the less complex shape models such as rectangular shape and pentagonal flat shape model have less equivalent stress than other models. Preferring the complex geometric shape like the lantern design requires more geometrical shape analysis and a more robust structure design for manufacturable jewelry. If the strength of the design is less critical for useability and the complex shape is desired, the designer can choose this type of shape. According to the analysis, if the maximum stress can be reduced by redesign or optimization, the pentagonal box design could be preferable.

According to the physical tensile test analysis, a significant tensile strength has been found in the XY-axis direction printing model rather than the Z-axis direction. The ANSYS analysis and tensile test results have found similar behavior during the experiment. The experiment shows the sufficient yield stress difference in printing orientation for all test

specimens except the pentagonal box. The specimen printed in XY orientation has been found greater tensile strength than the Z orientation specimen. If the design required tensile strength, it is recommended to choose the XY printing direction with a design like a lantern, pentagonal box. Therefore, this study observed that a critical geometric shape as twisted shape, helix shape visual quality was not satisfactory in XY printing direction. Consequently, according to the objective and idea, a designer can incorporate this study result during the design and production of jewelry.

Eventually, this study experimented on LED jewelry manufacturing with a pentagonal box design and figured out the production difficulties in processes. This experience could be a recommendation for the designer who is planning to design LED jewelry in a desktop 3D printer. A further study can be done on the shortcoming of LED jewelry and the kinematic jewelry design. This study designed a snap-fit join for assembling the link of jewelry; however, the detailed study has not yet been done, which can be established new lines for future studies.

LIST OF REFERENCES

1. ASTM Standard. Standard terminology for additive manufacturing technologies, vol. 10.04
2. Bikas, H., et al. "Additive Manufacturing Methods and Modelling Approaches: a Critical Review." *The International Journal of Advanced Manufacturing Technology*, vol. 83, no. 1-4, 2015, pp. 389–405., doi:10.1007/s00170-015-7576-2.
3. Fatma, Nosheen, et al. "Prospects of Jewelry Designing and Production by Additive Manufacturing." *Lecture Notes in Mechanical Engineering,* 2021, pp. 869–879., doi:10.1007/978-981-33-4795-3_80.
4. Cooper, Frank. "Sintering and Additive Manufacturing: 'Additive Manufacturing and the New Paradigm for the Jewellery Manufacturer.'" *Progress in Additive Manufacturing*, vol. 1, no. 1-2, 2016, pp. 29–43., doi:10.1007/s40964-015-0003-2.
5. Gebhardt, Andreas. *Understanding Additive Manufacturing*, 2011, doi:10.3139/9783446431621.fm.
6. Yap, Y.L., and W.Y. Yeong. "Additive Manufacture of Fashion and Jewellery Products: a Mini Review." *Virtual and Physical Prototyping*, vol. 9, no. 3, 2014, pp. 195–201., doi:10.1080/17452759.2014.938993.
7. Chua, C.K., Leong, K.F., and Lim, C.S. Rapid prototyping: principles and applications. 3rd ed. *Singapore: World Scientific Publishing*. 2010.
8. Somireddy, Madhukar, et al. "Development of Constitutive Material Model of 3D Printed Structure via FDM." *Materials Today Communications*, vol. 15, 2018, pp. 143–152., doi:10.1016/j.mtcomm.2018.03.004.
9. Ahn, Sung-Hoon, et al. "Anisotropic Material Properties of Fused Deposition Modeling ABS." *Rapid Prototyping Journal*, vol. 8, no. 4, 2002, pp. 248–257., doi:10.1108/13552540210441166.
10. Lee HB, Ko MSH, Gay RKL, Leong KF, Chua CK. 'Using computer-based tools, and technology to improve jewellery design and manufacturing.' *Int J Comput Appl Technol* 5:72–80. 1992. https://doi.org/10.1504/IJCAT.1992.062592
11. Yao, Tianyun, et al. "A Method to Predict the Ultimate Tensile Strength of 3D Printing Polylactic Acid (PLA) Materials with Different Printing Orientations." *Composites Part B: Engineering*, vol. 163, 2019, pp. 393–402., doi:10.1016/j.compositesb.2019.01.025.
12. Es-Said, O. S., et al. "Effect of Layer Orientation on Mechanical Properties of Rapid Prototyped Samples." *Materials and Manufacturing Processes*, vol. 15, no. 1, 2000, pp. 107–122., doi:10.1080/10426910008912976.

13. Sood, Anoop K., et al. "Experimental Investigation and Empirical Modelling of FDM Process for Compressive Strength Improvement." *Journal of Advanced Research*, vol. 3, no. 1, 2012, pp. 81–90., doi:10.1016/j.jare.2011.05.001.
14. "Abrighternite.com by LightUpYourLifeLLC on Etsy." *Etsy*, www.etsy.com/shop/LightUpYourLifeLLC?ref=l2-about-shopname. [Accessed: 2.04.21]
15. System, Nervous. "Kinematics Jewelry." *Projects by Nervous System*, n-e-r-v-o-u-s.com/projects/albums/kinematics-jewelry/#:~:text=Each%20Kinematics%20jewelry%20design%20is,a%20kind%20of%203D%20printing. [Accessed: 2.04.21]
16. Nervous System, inc. *Nervous System*, n-e-r-v-o-u-s.com/index.php. [Accessed: 2.04.21]
17. Wohlers T,2015, *Wohlers Report 2015: Global Reports, Wohlers Associates, Belgium*.
18. "3D Printing Technology in the Jewelry Sector." Edited by 3DA, *3D Adept Media*, 29 Apr. 2019, 3dadept.com/3d-printing-technology-in-the-jewellery-sector/. [Accessed: 29.03.2021]
19. Kianian, Babak. *Wohlers Report 2016: 3D Printing and Additive Manufacturing State of the Industry, Annual Worldwide Progress Report: Chapter title: The Middle East* 21 udg. FORT COLLINS, COLORADO, USA: Wohlers Associates, Inc. 2016.
20. "Twice as Many 3D Printers Shipped over 2016, Gartner Predicts." *3ders.Org*, www.3ders.org/articles/20161013-twice-as-many-3d-printers-shipped-over-2016-gartner-predicts.html. [Accessed: 29.03.2021]
21. Strong, Brad. "3D Printers Under $4000 Compared for Industrial Usage." *TransMagic*, 15 Mar. 2019, transmagic.com/3d-printers-under-4000-compared-for-industrial-usage/?fbclid=IwAR2Oq8shb37hgM2cJCXOpB7d3mHffpYXxWk_WI9dVAZgxMh5qI4leV9Z6hI. [Accessed: 29.03.2021]
22. Wise, David. "Best 3D Printer of 2021." *TechGearLab*, TechGearLab, 11 May 2021, www.techgearlab.com/topics/cool-gadgets/best-3d-printer/. [Accessed: 29.03.2021]
23. Published by Statista Research Department, and Apr 29. "Global 3D Printing Industry Market Size." *Statista*, 29 Apr. 2021, www.statista.com/statistics/315386/global-market-for-3d-printers/. [Accessed: 6.01.2021]
24. "2021 Best Sites for Free STL Files & 3D Printer Models." *All3DP*, 22 Apr. 2021, all3dp.com/1/free-stl-files-3d-printer-models-3d-print-files-stl-download/?fbclid=IwAR1iOZ9RDqOmWDp_ItnxhnY2818TJ6wBAGJXQuxrspJi601Th9z3Ylx_Fjo. [Accessed: 6.01.2021]

25. Thompson, Mary Kathryn, et al. "Design for Additive Manufacturing: Trends, Opportunities, Considerations, and Constraints." *CIRP Annals*, vol. 65, no. 2, 2016, pp. 737–760., doi:10.1016/j.cirp.2016.05.004.
26. "Wax 3D Printing Helps Uptown Diamond Craft A Gem." *3D Systems*, 29 Mar. 2021, www.3dsystems.com/learning-center/case-studies/projetr-3510-cpx-3d-printer-gem-uptown-diamond-jewelry. [Accessed: 6.01.2021]
27. "Iris Van Herpen Debuts Wearable 3D Printed Pieces at Paris Fashion Week." *Materialise*,www.materialise.com/cases/iris-van-herpen-debuts-wearable-3d-printed-pieces-at-paris-fashion-week. [Accessed: 6.01.2021]
28. "Kipling: No Monkey Business." *Materialise*, www.materialise.com/cases/kipling-no-monkey-business. [Accessed: 6.01.2021]
29. 3dsourced. "Top 10 Most Stunning 3D Printed Jewelry Pieces 2021." *3DSourced*, 4 Jan. 2021, www.3dsourced.com/rankings/3d-printed-jewelry/. [Accessed: 29.03.2021]
30. *Ender-3 3D Printer*, www.creality.com/goods-detail/ender-3-3d-printer. [Accessed: 3.05.2021]
31. "PrusaSlicer & Ender 3: The Best Profile." *All3DP*, 19 Apr. 2021, all3dp.com/2/prusaslicer-ender-3-best-profile/. [Accessed: 3.05.2021]
32. "Replicator Z18 Professional 3D Printer." *MakerBot*, www.makerbot.com/3d-printers/replicator-z18/. [Accessed: 3.05.2021]
33. S. S. Crump, "Apparatus and method for creating three-dimensional objects," U.S. Patent No. 5121329, June 9, 1992.
34. Mwema, Fredrick Madaraka, and Esther Titilayo Akinlabi. "Basics of Fused Deposition Modelling (FDM)." *Fused Deposition Modeling*, 2020, pp. 1–15., doi:10.1007/978-3-030-48259-6_1.
35. Singh, R., et al. "Implant Materials and Their Processing Technologies." *Reference Module in Materials Science and Materials Engineering*, 2016, doi:10.1016/b978-0-12-803581-8.04156-4.
36. Camargo, José C., et al. "Mechanical Properties of PLA-Graphene Filament for FDM 3D Printing." *The International Journal of Advanced Manufacturing Technology*, vol. 103, no. 5-8, 2019, pp. 2423–2443., doi:10.1007/s00170-019-03532-5.
37. Liao, Yuhan, et al. "Erratum: Effect of Porosity and Crystallinity on 3D Printed PLA Properties. Polymers 2019, 11, 1487." *Polymers*, vol. 12, no. 1, 2020, p. 142., doi:10.3390/polym12010142.
38. "Slicer Settings: The Most Important Settings to Get Started." *All3DP*, 18 Mar. 2021, all3dp.com/2/3d-slicer-settings-3d-printer. [Accessed: 8.05.21]
39. "PrusaSlicer & Ender 3: The Best Profile." *All3DP*, 19 Apr. 2021, all3dp.com/2/prusaslicer-ender-3-best-profile/. [Accessed: 8.05.21]

40. Thingiverse.com. "Kinematics @ Home Bracelets by Nervoussystem." *Thingiverse*, www.thingiverse.com/thing:195497. [Accessed: 5.05.21]
41. "Shop for Handmade, Vintage, Custom, and Unique Gifts for Everyone." *Etsy*, www.etsy.com/. [Accessed: 29.03.2021]
42. "RADIAN Design | 3D Printed Jewelry and Sustainable Home Goods." *RADIAN*, radian-design.com/. [Accessed: 29.03.2021]
43. "Diana Law." *Diana Law Printed Accessories*, www.dianalaw.com/. [Accessed: 29.03.2021]
44. Single Sided Cube Ring, "GUY&MAX: Fine Jewellery Designers & Makers." *GUY&MAX,* Fine Jewellery Designers & Makers, guyandmax.com/. [Accessed: 29.03.2021]
45. *Pearls: Necklaces, Rings, Earrings, Bracelets, Sets*, www.americanpearl.com/. [Accessed: 29.03.2021]
46. "Anna Reikher on Etsy." *Etsy*, www.etsy.com/people/annareik. [Accessed: 29.03.2021]
47. "Jewelry 3D Printing." *Shapeways*, 6 May 2021, www.shapeways.com/industry/jewelry. [Accessed: 29.03.2021]
48. *Universal Testing Machines*, www.iitk.ac.in/smc/universal-testing-machines. [Accessed: 19.05.2021]

APPENDICES

Appendix 1 Tensile test result of the pentagonal box

Product	: ehe	**Load Range**	: 1000 N
Batch	:	**Extension Range**	: 3,000 mm
Date	: 19.05.2021	**Gauge Length**	: 1,000 mm
Operator	:	**Speed**	: 1,000 mm/min
		Approach Speed	: 0,1000 mm/min
		Preload	: 0 N

No.	Yield Force N	Elong at Yield %	Max Force N	Elong at Max %	Force at Break N
1	31,70	45,75	31,70	45,8	0,30
2	36,70	60,00	36,70	60,0	20,30
3	11,70	15,00	28,00	387,8	11,30
4	35,00	48,00	35,00	48,0	11,70
5	39,00	49,00	39,00	49,0	7,30
6	39,70	45,00	39,70	45,0	5,70
Mean	32,30	43,79	35,02	105,9	9,43
Median	35,85	46,88	35,85	48,5	9,30
Maximum	39,70	60,00	39,70	387,8	20,30
Minimum	11,70	15,00	28,00	45,0	0,30

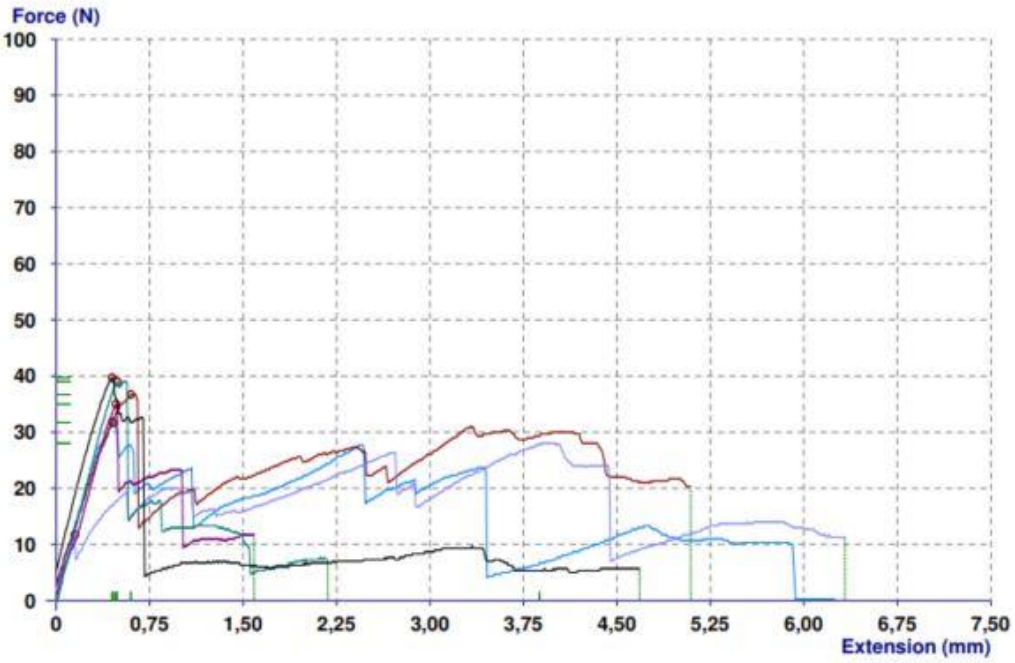

- Page 1 -

Appendix 2 Tensile test result of the lantern shape

Product	: ehe	**Load Range**	: 1000 N
Batch	:	**Extension Range**	: 3,000 mm
Date	: 19.05.2021	**Gauge Length**	: 1,000 mm
Operator	:	**Speed**	: 1,000 mm/min
		Approach Speed	: 0,1000 mm/min
		Preload	: 0 N

No.	Yield Force N	Elong at Yield %	Max Force N	Elong at Max %	Force at Break N
1	372,4	145,0	372,4	145,0	36,80
2	356,8	116,3	376,8	135,0	38,40
3	285,6	95,2	304,8	121,6	38,80
4	72,3	32,6	72,3	32,6	9,69
5	72,7	25,0	72,7	25,0	7,30
6	56,3	18,0	56,3	18,0	5,70
Mean	202,7	72,0	209,2	79,5	22,78
Median	179,2	63,9	188,8	77,1	23,25
Maximum	372,4	145,0	376,8	145,0	38,80
Minimum	56,3	18,0	56,3	18,0	5,70

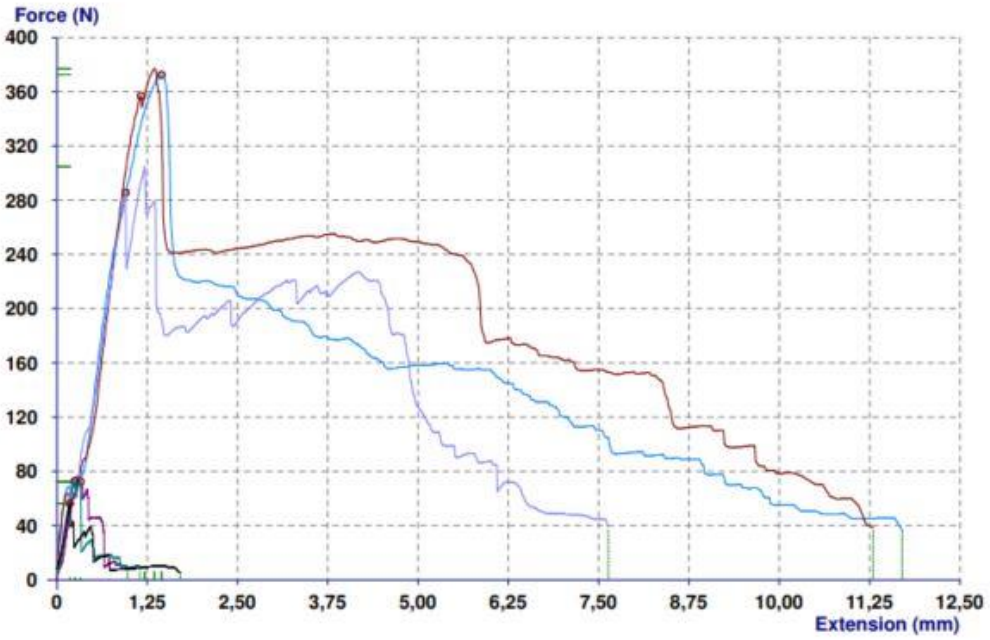

Appendix 3 Tensile test result of the helix shape

Product	: ehe	**Load Range**	: 1000 N
Batch	:	**Extension Range**	: 1,000 mm
Date	: 19.05.2021	**Gauge Length**	: 10,00 mm
Operator	:	**Speed**	: 1,000 mm/min
		Approach Speed	: 1,000 mm/min
		Preload	: 0 N

No.	Yield Force N	Elong at Yield %	Max Force N	Elong at Max %	Force at Break N
1	53,00	4,300	105,4	21,50	104,4
2	39,38	2,900	117,4	21,00	116,6
3	49,00	3,600	97,3	16,90	97,0
4	6,30	4,400	6,3	4,40	0,3
5	5,66	0,210	26,3	3,07	7,3
6	28,34	1,940	43,0	5,81	38,7
Mean	30,28	2,892	65,9	12,11	60,7
Median	33,86	3,250	70,2	11,36	67,8
Maximum	53,00	4,400	117,4	21,50	116,6
Minimum	5,66	0,210	6,3	3,07	0,3

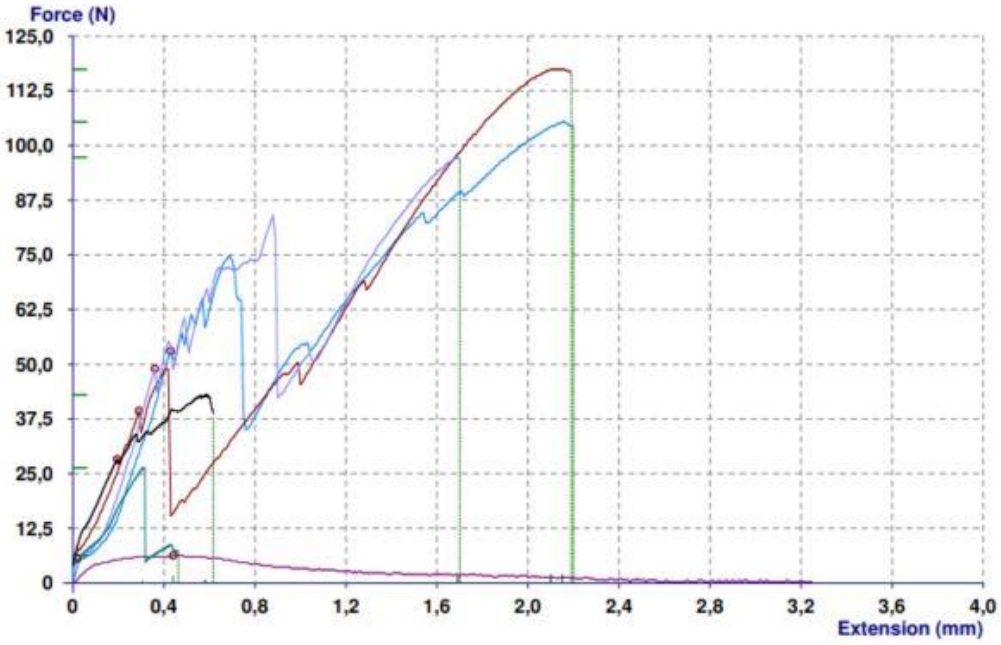

- Page 1 -

Appendix 4 Tensile test result of the twisted shape

Product	: ehe	**Load Range**	: 100,0 N
Batch	:	**Extension Range**	: 3,000 mm
Date	: 17.05.2021	**Gauge Length**	: 50,00 mm
Operator	:	**Speed**	: 5,000 mm/min
		Approach Speed	: 2,000 mm/min
		Preload	: 0 N
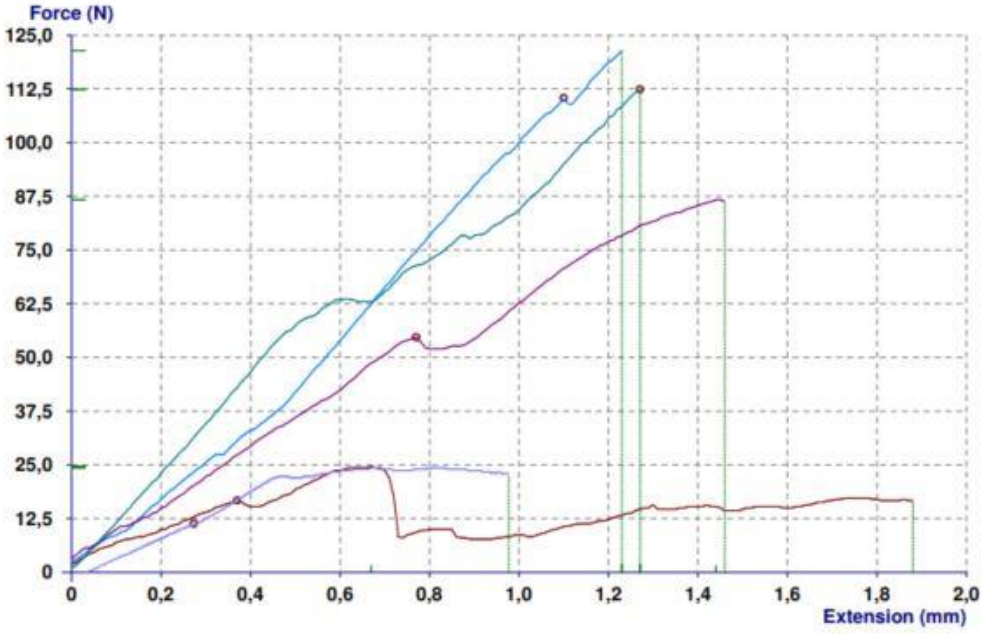
No.	Yield Force N	Elong at Yield %	Max Force N	Elong at Max %	Force at Break N
1	110,4	2,200	121,4	2,460	121,4
2	16,7	0,740	24,7	1,340	16,7
3	11,3	0,546	24,3	1,338	23,0
4	54,7	1,540	86,7	2,880	86,3
5	112,4	2,541	112,4	2,541	112,4
Mean	61,1	1,513	73,9	2,112	71,9
Median	54,7	1,540	86,7	2,460	86,3
Maximum	112,4	2,541	121,4	2,880	121,4
Minimum	11,3	0,546	24,3	1,338	16,7